CBPF-NF-053/95
TAUP 2283/95
hep-ph 9509286

Shadowing Corrections in Diffractive QCD Leptoproduction of Vector Mesons

E. Gotsman [a)*] *E.M. Levin* [b) c)†] *and U. Maor* [a) b)‡]
a) School of Physics and Astronomy
Raymond and Beverly Sackler Faculty of Exact Sciences
Tel Aviv University, Tel Aviv 69978, ISRAEL

b) LAFEX, Centro Brasileiro de Pesquisas Físicas (CNPq)
Rua Dr. Xavier Sigaud 150, 22290 - 180 Rio de Janeiro, RJ, BRASIL

c) Theory Department, Petersburg Nuclear Physics Institute
188350, Gatchina, St. Petersburg, RUSSIA

Abstract

The formulae for shadowing corrections in deep inelastic leptoproduction of vector mesons are presented. These formulae are also applicable for photoproduction of vector mesons constituted of heavy quarks. Our results are conveniently presented by the definition of a damping factor giving the reduction of the calculated cross sections due to shadowing. Our calculated cross sections are compared with those obtained with no shadowing and with the available experimental data including the recent data from HERA. We have also investigated the importance of shadowing on the relationship between $\frac{\partial F_2(Q^2,x)}{\partial \ln Q^2}$ and the cross section for virtual photoproduction of vector mesons. A discussion of shadowing corrections to the proton's gluon density is presented and numerical estimates are given.

Key-words: Perturbative QCD; Diffraction dissociation; Shadowing corrections; HERA experimental data.

*e-mail: gotsman@ccsg.tau.ac.il
†e-mail: levin@lafex.cbpf.br
‡e-mail: maor@vm.tau.ac.il

CBPF-NF-053/95

1 Introduction

Over the last decade, following the paper of Bartels and Loewe[1], diffractive leptoproduction of vector mesons has been investigated within the framework of perturbative QCD (pQCD). In particular, it has been shown[1,2] that the DIS cross sections can be calculated in pQCD provided that both the energy and photon virtuality are large enough. These cross sections are proportional to $(xG(Q^2,x))^2$, where $xG(Q^2,x)$ is the gluon distribution within the nucleon target. Futhermore, Donnachie and Landshoff[3] have shown in a non perturbative Pomeron approach, that both the initial photon and the produced vector meson have to be longitudinally polarized to realize the leading Q^2 behaviour of the cross section i.e. $\frac{d\sigma}{dt} \propto \frac{1}{Q^4}$. This result has also been confirmed in the BFKL approach to the Pomeron structure in pQCD[4]. A new insight into the problem has been suggested by Ryskin[5], who proved that J/ψ leptoproduction can be calculated reliably in the leading log approximation (LLA) of pQCD, and that the non-perturbative effects coming from large distances, can be factored out in terms of the wave function of the produced vector meson at the origin. In addition, Ryskin pointed out that the pQCD calculation is also valid for leptoproduction of light vector mesons. For heavy vector mesons the calculation can be safely continued to $Q^2 = 0$. An important contribution in the construction of this formalism appears in the paper of Kopeliovich et.al.[6], where the wave function for the light vector mesons is evaluated using the constituent quark model. Finally, we mention the contribution of Brodsky et.al.[7] who showed how to factor out the long distance effects for the case of light vector mesons in terms of the light-cone $\bar{q}q$ wave function of the produced vector meson[8].

The goal of this paper is to study the shadowing (screening) corrections (SC) for lepto and photoproduction of vector meson. To this end we shall generalize the formalism developed by Mueller[9] for the gluon and quark densities. Technically, we shall utilize the idea of a $r_\perp$- representation for the SC suggested in Ref.[10] and further discussed in Refs.[6,9,11,12]. The quantity we wish to calculate is the damping factor defined in our previous publication[13] as:

$$D^2 \;=\; \frac{\frac{d\sigma(\gamma^* p \to VP)}{dt}[\; with \;\; SC]}{\frac{d\sigma(\gamma^* p \to Vp)}{dt}[\; without \;\; SC]} \;|_{t=0} \qquad (1)$$

where $t = -q_\perp^2$ denotes the square of momentum transfer in the reaction $\gamma^* p \to Vp$.

The structure of our paper is as follows: In section 2 we define our notation and numerical coefficients pertinent to the DIS production of vector mesons without including SC. Basically, we reproduce the well known results of Refs.[5,7], doing calculations in the $r_\perp$-representation ($r_\perp$ denotes the transverse separation between the quark and antiquark).

We will show that the results hold, not only in the leading log of the GLAP evolution equations [14], but also in the leading $\ln\frac{1}{x}$ approximation of pQCD, as was pointed out by Ryskin[5]. In section 3 we extend the formalism suggested by Levin and Ryskin[10] and Mueller[9] to the case of a $\bar{q}q$ pair with a definite value of $r_\perp$ transversing the target

(be it a proton or nucleus). We will show that for vector meson production we obtain a closed expression for the damping factor. Our result does not depend on the large transverse distances, allowing us to calculate the SC to a good theoretical accuracy in pQCD. In the fourth section we prove that the damping factor can be rewritten using the experimentally measured value of $\frac{\partial F_2(Q^2,x)}{\partial \ln Q^2}$. To this end, we use the leading log $\frac{1}{x}$ approximation of pQCD with a variety of shadowing corrections. In section 5 we discuss the SC for the gluon distribution, and investigate the uncertainties due to large distance contributions which can be important for this case. Section 6 contains the numerical evaluations of our formalism, which are compared with those obtained for the case with no SC. Our results are then compared with the experimental data, mostly from HERA. A summary and final discussion are presented in section 7.

2 Vector meson production in DIS without shadowing corrections

2.1 Notations

In this paper we will use the following notations (see Fig.1):

Q^2 denotes the virtuality of the photon in DIS, m_V is the mass of the produced vector meson and m is the target mass assumed to be a proton unless specified otherwise.

$x = \frac{Q^2+m_V^2}{s}$, where $\sqrt{s}$ is the c.m. energy of the incoming photon-proton system.

$a^2 = z(1-z)\,Q^2 + m_Q^2$, where z is the fraction of of the photon energy carried by the quark. m_Q is the mass of the current quark.

$\vec{k}_\perp$ denotes the transverse momentum of the quark, and $\vec{r}_\perp$ the transverse separation between the quark and antiquark.

$\vec{b}_\perp$ is the impact parameter of our reaction which is the variable conjugate to the momentum transfer ($\vec{q}_\perp$).

$\vec{l}_{i\perp}$ denote the transverse momentum of the gluons attached to the quark-antiquark pair (see Fig.1).

We will use the evolution equations for the parton densities in the moment space. For any function $f(x)$, we define a moment $f(\omega)$

$$f(\omega) = \int_0^1 dx\; x^\omega\; f(x) \quad . \tag{2}$$

Note that, the moment variable ω, is chosen such that the $\omega = 0$ moment measures the number of partons, and the $\omega = 1$ moment measures their momentum. An alternative moment variable N defined such that $N = \omega + 1$, is often found in the literature.

The x - distribution can be reconstructed by considering the inverse Mellin transform. For example, for the gluon distribution it reads

$$xG(Q^2,x) \;=\; \frac{1}{2\pi i}\int_C d\omega\; x^{-\omega}\; g(Q^2,\omega)\;. \tag{3}$$

The contour of integration C is taken to the right of all singularities. The solutions to both the GLAP and the BFKL equations have the general form

$$g(Q^2,\omega) \;=\; g(\omega)\, e^{\gamma(\omega) ln Q^2}\;, \tag{4}$$

where $\gamma(\omega)$ denotes the anomalous dimension, which in the leading $\ln\frac{1}{x}$ approximation of pQCD, is a function of $\frac{\alpha_S}{\omega}$ and can be presented as the following series[15]

$$\gamma(\omega) \;=\; \frac{\alpha_S N_c}{\pi}\frac{1}{\omega} \;+\; \frac{2\alpha_S^4 N_c^4 \zeta(3)}{\pi^4}\frac{1}{\omega^4} \;+\; O(\frac{\alpha_S^5}{\omega^5})\;. \tag{5}$$

Our amplitude is normalized such that

$$\frac{d\sigma}{dt} \;=\; \pi\,|f(s,t)|^2\;,$$

$$\sigma_{tot} \;=\; 4\pi\; Im\, f(s,0)\;.$$

The scattering amplitude in $b_\perp$-space is defined as

$$a(s,b_\perp) \;=\; \frac{1}{2\pi}\int d^2q_\perp\; e^{-i\vec{q}_\perp\cdot\vec{b}_\perp}\; f(s,t=-q_\perp^2)\;.$$

In this representation

$$\sigma_{tot} \;=\; 2\int d^2b_\perp\; Im\; a(s,b_\perp)\;,$$

$$\sigma_{el} \;=\; \int d^2b_\perp\;|\,a(s,b_\perp)|^2\;.$$

In general we have attempted to adjust our notation and normalization to agree with those of Brodsky et.al.[7].

2.2 The amplitude in the $r_\perp$ representation

This approach was originally formulated in Ref.[10] and has been carefully developed in Ref.[9]. While the boson projectile is transversing the target, the distance $r_\perp$ between the quark and antiquark can vary by an amount $\Delta r_\perp \;\propto R\,\frac{k_\perp}{E}$, where E denotes the energy of the pair in the target rest frame, and R is the size of the target (see Fig.1). The quark transverse momentum is $k_\perp \;\propto\; \frac{1}{r_\perp}$. Therefore

$$\Delta r_\perp \;\propto\; R\frac{k_\perp}{E} \;\ll\; r_\perp\;, \tag{6}$$

which is valid if

$$r_\perp^2 \cdot s \gg 2m\,R\,, \tag{7}$$

where $s \simeq 2mE$. The above condition has the following form in terms of x

$$x \ll \frac{1}{2mR}\,. \tag{8}$$

Hence, at small values of x, the transverse distance between the quark and antiquark is a good degree of freedom[9,10,16], and the interaction of a virtual photon with the target can be written in the form (we use the notation of Ref.[7])

$$M_f = \sqrt{N_f}\sum_{\lambda_1\,\lambda_2}\int_0^1 dz \int \frac{d^2r_\perp}{2\pi}\;\Psi^{\gamma^*}(Q^2,r_\perp,z)\;\sigma(r_\perp,q_\perp^2)\;[\Psi^V(r_\perp,z)]^*\,, \tag{9}$$

where λ_i denotes the polarization of the quarks. Note that both γ^* and V are longitudinally polarized. Ψ^V denotes the wave function of the produced vector meson, and we anticipate that the value of $r_\perp$ that dominates the integral in Eq.(9) will be small (of the order of $r_\perp \propto \frac{1}{Q}$). The form of Ψ^{γ^*}, the wave function of the longitudinally polarized photon, has been given in Ref.[17], i.e.

$$\Psi^{\gamma^*}(r_\perp,z) = Qz(1-z)K_0(\,a\,r_\perp\,)\,. \tag{10}$$

$\sigma(r_\perp,q_\perp^2)$ is the cross section of the $\bar{q}q$ pair with a transverse separation $r_\perp$ which scatter off the target with momentum transfer $q_\perp$. We first evaluate it at $q_\perp = 0$.

2.3 $\sigma(r_\perp,q_\perp^2)$ at $q_\perp = 0$

The expression for $\sigma(r_\perp,q_\perp^2)$ at $q_\perp = 0$, was first written down in Ref.[10] (see Eq.(8) of this paper). It turns out that σ can be expressed through the unintegrated parton density ϕ first introduced in the BFKL papers[18] and widely used in Ref.[2]. The relation of this function to the Feynman diagrams and the gluon distribution can be calculated using the following equation:

$$\alpha_S(Q^2)\cdot xG(Q^2,x) = \int^{Q^2} dl_\perp^2\;\alpha_S(l_\perp^2)\;\phi(l_\perp^2,x)\,. \tag{11}$$

Using the above equation we reproduce the results of Ref.[10], which reads

$$\sigma(r_\perp,q_\perp^2) = \frac{16C_F}{N_c^2-1}\,\pi^2\int\phi(l_\perp^2,x)\,\{\;1\;-\;e^{i\vec{l}_\perp\vec{r}_\perp}\;\}\;\frac{\alpha_S(l_\perp^2)}{2\pi}\,\frac{d^2l_\perp}{l_\perp^2}\,, \tag{12}$$

where $\phi = \frac{\partial xG(Q^2,x)}{\partial Q^2}$ and $C_F = \frac{N_c{}^2-1}{2N_c}$. We evaluate this integral using Eqs.(3,4) and integrate over the azimuthal angle. Introducing a new variable $\xi = r_\perp l_\perp$, the integral can be written in the form

$$\sigma(r_\perp,q_\perp^2) = \frac{16C_F\alpha_S}{N_c^2-1}\,\pi^2\int_C\frac{d\omega}{2\pi i}\;g(\omega)\;\gamma(\omega)\;(r_\perp^2)^{1-\gamma(\omega)}\int_0^\infty d\,\xi\;\frac{1-J_0(\xi)}{(\xi)^{3-2\gamma(\omega)}}\,. \tag{13}$$

Evaluating the integral over ζ (see Ref.[19] **11.4.18**) we have

$$\sigma(r_\perp, q_\perp^2) \;=\; \frac{8C_F\alpha_S}{N_c^2-1}\,\pi^2\int_C \frac{d\omega}{2\pi i}\; g(\omega)\;\gamma(\omega)\;(\frac{r_\perp^2}{4})^{1-\gamma(\omega)}\;\frac{\Gamma(\gamma(\omega)\;\Gamma(1-\gamma(\omega))}{(\,\Gamma(2-\gamma(\omega)\,)^2}\;. \qquad (14)$$

In the double log approximation of pQCD, where $\gamma(\omega) \ll 1$, the cross section for $N_c = N_f = 3$ reads

$$\sigma(r_\perp, q_\perp^2) \;=\; \frac{\alpha_S(\frac{4}{r_\perp^2})}{3}\,\pi^2\,r_\perp^2\,\left(\; xG^{GLAP}(\frac{4}{r_\perp^2}, x)\;\right)\;. \qquad (15)$$

This result coincides with the value of the cross section given in Refs.[6,20], (if we neglect the factor 4 in the argument of the gluon density). We checked that Eq.(2.16) of Ref.[7] also leads to the same answer, unlike the value for σ quoted in Ref.[7] (see Eq.(2.20)) which differs from ours by a factor of 2.

We do not want to make use of the double log approximation, which corresponds to the first term in the expansion given in Eq.(5), and prefer to use the complete series for $\gamma(\omega)$. Indeed, all diagrams in which an extra gluon goes from the bottom to the top as well as from left to right of the diagram of Fig.1 (see also Fig.2) do not produce an extra power of $\ln\frac{1}{x}$. They only give corrections of the order α_S either to the anomalous dimension, or to the coefficient function. Calculating in the $\ln\frac{1}{x}$ approximation, considering $\frac{\alpha_S}{\omega} \gg \alpha_S$ in the region of small x, we can safely use the value of the anomalous dimension given in Eq.(5). From Eq.(14) one can directly obtain the simple answer in another limiting case, namely, when $\gamma(\omega) \to \frac{1}{2}$. This limit corresponds to the solution of the BFKL evolution equation[18] in the diffusion region when $\ln\frac{4}{r_\perp^2} \leq \sqrt{\alpha_S \ln\frac{1}{x}}$. Neglecting the deviation of γ from $\frac{1}{2}$ we get

$$\sigma(r_\perp, q_\perp^2) \;=\; \frac{2\alpha_S}{3}\,\pi^2\,r_\perp^2\,\left(\; xG^{BFKL}(\frac{4}{r_\perp^2}, x)\;\right)\;. \qquad (16)$$

In the intermediate range of Q^2 and x, we cannot obtain a simple formula for σ in terms of the gluon density. We stress that a difference of a factor of two in σ does not mean that the cross section of vector meson production will change by a factor four. The BFKL density behaves as $r_\perp F(\ln r_\perp^2, x)$, and the integral over $r_\perp$ will be different for the double log approximation and for BFKL. We will consider these two cases and will integrate over $r_\perp$ to see how big the difference is in the final answer.

2.4 The amplitude of vector meson production at $q_\perp = 0$

We wish to calculate the amplitude for vector meson production, using Eq.(9). To do this we use the integral representation for the McDonald function[19] and rewrite Eq.(10) in the form

$$\Psi^{\gamma^*}(r_\perp, z) \;=\; \frac{Qz(1-z)}{2}\;\int_0^\infty \frac{dt}{t}\;exp\left(-\frac{1}{2}[t + \frac{a^2\,r_\perp^2}{t}]\right)\;. \qquad (17)$$

Substituting Eqs.(14,16) in Eq.(9) we obtain

$$M_f \;=\; \sqrt{N_f}\sum_{\lambda_1\,\lambda_2}\int_0^1 dz\int\frac{d^2r_\perp}{2\pi}\;\frac{Qz(1-z)}{2}\int_0^\infty\frac{dt}{t}\;exp\left(-\frac{1}{2}[t + \frac{a^2\,r_\perp^2}{t}]\right) \qquad (18)$$

$$\frac{8C_F\alpha_S}{N_c^2-1}\,\pi^2\int_C\frac{d\omega}{2\pi i}\,g(\omega)\,\gamma(\omega)\,(\frac{r_\perp^2}{4})^{1-\gamma(\omega)}\;\frac{\Gamma(\gamma(\omega)\,\Gamma(1-\gamma(\omega))}{(\,\Gamma(2-\gamma(\omega)\,)^2}\,[\Psi^V(r_\perp,z)]^*\;.$$

Anticipating that the typical value of $r_\perp$ in the integral will be small ($r_\perp\,\propto\,\frac{1}{Q}$), we can replace the hadron wave function by its value at $r_\perp=0$. Introducing a new variable $\zeta\;=\;\frac{a^2r_\perp^2}{2t}$, we integrate over $r_\perp^2$ and t. It is easy to see that the integral corresponds to $\zeta\;\simeq\;1$ and $t\;\simeq\;2$. This means that the typical value of $r_\perp^2$ is of the order of $\frac{4}{a^2}\;\ll\;1$. This justifies our assumption that the wave function of a produced hadron enters at small $r_\perp$. The final general answer is

$$M_f\;=\;\sqrt{N_f}\,\sum_{\lambda_1\,\lambda_2}\int_0^1 d\,z\;\;\frac{Qz(1-z)}{2}\;\frac{8C_F\alpha_S}{N_c^2-1}\;\pi^2\int_C\frac{d\omega}{2\pi i}\;g(\omega)\qquad(19)$$

$$\frac{16}{a^4}\;(a^2)^{\gamma(\omega)}\;\Gamma(1+\gamma(\omega))\;\Gamma(1-\gamma(\omega))\;[\Psi^V(r_\perp=0,z)]^*\;.$$

In the case of the GLAP approach we can simplify Eq.(19) by considering $\gamma(\omega)\;\ll\;1$, while for BFKL the simplification occurs when $\gamma(\omega)\;\rightarrow\;\frac{1}{2}$. One can see that there is a difference of $\pi/2$ in the amplitude, but the final estimate is obtained only after integration over z.

We can approximate the integration over z by putting $z=\frac{1}{2}$ in the $\ln a^2$

dependence of the density. This gives

$$M_f\;=\;CQ\;\alpha_S\left(\,xG^{GLAP}(a^2(z=\frac{1}{2}),x)\right)\;\int_0^1 d\,z\;\frac{z(1-z)}{a^4}[\Psi^V(0,z)]^*\;,\qquad(20)$$

for the GLAP equations, while for the BFKL we get

$$M_f\;=\;C\,Q\,\alpha_S\,\frac{\pi}{2}\left(xF^{BFKL}(\ln a^2(z=\frac{1}{2}),x)\right)\;\int_0^1 d\,z\;\frac{z(1-z)}{a^3}[\Psi^V(0,z)]^*\;,\qquad(21)$$

where we have replaced the BFKL gluon distribution by $xG^{BFKL}(a^2,x)=\frac{r_\perp}{R}\cdot F(\ln r_\perp^2,x)$ as discussed above. In the above equations we have replaced all constants by the coefficient C.

The function $\Psi^V(0,z)$ is just the function which has been introduced in Ref.[7] (see Eq.(2.25) there). Using the asymptotic form of the z-dependence, namely $\Psi^V\;\propto z(1-z)$ for the case of massless quarks, we have:

$$M_f\;=\;C\,\frac{\alpha_S}{Q^3}\left(xG^{GLAP}(\frac{Q^2}{4},x)\right)\;,\qquad(22)$$

$$M_f\;=\;C\,\frac{\alpha_S}{Q^3}\,\frac{\pi^2}{8}\left(xG^{BFKL}(\frac{Q^2}{4},x)\right)\;.\qquad(23)$$

Consequently, the difference in the value of the amplitude turns out to be rather small, about 25%. We note that the BFKL equation gives the anomalous dimension close to $\frac{1}{2}$, which only generates a $\frac{1}{Q^2}$ behaviour of the amplitude, while the GLAP equations give $\frac{1}{Q^3}$ for the same value. In the nonrelativistic case the difference is $\pi/2$ in favour of the BFKL equation.

2.5 The $b_\perp$ dependence of the amplitude

To deal with the SC we need to know the amplitude not only at $q_\perp$=0, but also at all values of momentum transfer, so that we can calculate the profile function of the amplitude in impact parameter space. The gluon density has a week dependence on $q_\perp$ at small values of $q_\perp$, both in the double log approximation (see Ref.[2]) as well as for the BFKL approach (see Ref.[20]). Therefore, the $q_\perp$-dependences come from the form factor of the $\bar{q}q$ pair with a transverse separation $r_\perp$, and the form factor of the proton target.

The target form factor is not treated theoretically in pQCD, and that for our purpose we assume the exponential parameterization for it will suffice, namely

$$F_p(q_\perp^2) \;=\; e^{-\frac{B}{4}\,q_\perp^2}\;.$$

If we put the Pomeron slope α'=0 the slope B can be extracted from the experimental data on hadron-hadron collisions. Namely, $B = B_{el}^{pp}(\alpha'=0)$, where B_{el} is the slope of the differential cross section of proton-proton collision. For the numerical estimates we use phenomenological information to extract the value of B [21]. The value of B defined in this way, is very close to the one obtained from the proton electromagnetic form factor.

The form factor of the $\bar{q}q$ pair with a transverse separation $r_\perp$ is equal to

$$F_{\bar{q}q}(q_\perp^2) \;=\; \Psi^i_{\bar{q}q}\left(\frac{(\vec{k}_{1\perp} \;-\; \vec{k}_{2\perp})\cdot\vec{r}_\perp}{2}\right)\,\Psi^{f*}_{\bar{q}q}\left(\frac{(\vec{k'}_{1\perp} \;-\; \vec{k'}_{2\perp})\cdot\vec{r}_\perp}{2}\right)\;, \qquad (24)$$

where k_i (k'_i) denotes the momentum of the i quark before and after the collision. Each of the wave functions has an exponential form, and a simple sum of different attachments of gluon lines to quark lines gives

$$F_{\bar{q}q}(q_\perp^2) \;=\; e^{i\frac{\vec{q}_\perp\cdot\vec{r}_\perp}{2}}\;\{\;1 \;-\; e^{i\vec{l}_\perp\cdot\vec{r}_\perp}\;\}\;. \qquad (25)$$

We have absorbed the last factor in the expression for the cross section, while the first one gives the $q_\perp$ dependence of the $\bar{q}q$ form factor, which after integration over the azimuthal angle has the form

$$F_{\bar{q}q}(q_\perp^2) \;=\; J_0(\frac{q_\perp\;r_\perp}{2})\;. \qquad (26)$$

To calculate further, we need the profile function in $b_\perp$ space, which is defined as

$$S(b_\perp^2) \;=\; \frac{1}{4\pi^2}\int d^2q_\perp\; e^{i\vec{b}_\perp\cdot\vec{q}_\perp}\;F_p(q_\perp^2)\;F_{\bar{q}q}(q_\perp^2)\;. \qquad (27)$$

An exact computation gives

$$S(b_\perp^2) \;=\; \frac{1}{\pi B}\,I_0\left(\frac{b_\perp\;r_\perp}{B}\right)\;e^{-\frac{b_\perp^2\;+\;\frac{r_\perp^2}{4}}{B}}\;. \qquad (28)$$

To simplify the calculation we replace the above function by

$$S(b_\perp^2) \;=\; \frac{1}{\pi B'}\,e^{-\frac{b_\perp^2}{B'}}\;, \qquad (29)$$

where

$$B' \;=\; B\left(1 \;+\; \frac{r_\perp^2}{4B}\right) \;\simeq\; B\left(1 \;+\; \frac{1}{a^2B}\right)\;.$$

Eq.(29), in the small $b_\perp^2$ expansion, has the same radius as in Eq.(28).

3 Shadowing corrections to diffractive leptoproduction of vector mesons

3.1 Percolation of a $\bar{q}q$-pair through the target.

To calculate the shadowing corrections we follow the procedure suggested in Refs.[9,10,13,21]. Namely, we replace $\sigma(r_\perp, q^2_\perp = 0)$ in Eq.(9) by

$$\sigma^{SC}(r_\perp) \;=\; 2 \int d^2 b_\perp \left(1 \;-\; e^{-\frac{1}{2}\,\sigma(r_\perp, q^2_\perp = 0)\; S(b^2_\perp)} \right) . \tag{30}$$

The above formula is a solution of the s-channel unitarity relation

$$2\; Im\, a(s, b_\perp) \;=\; |a(s, b_\perp)|^2 \;+\; G_{in}(s, b_\perp) \, , \tag{31}$$

where a denotes the elastic amplitude for the $\bar{q}q$ pair with a transverse separation $r_\perp$, and G_{in} is the contribution of all the inelastic processes. The inelastic cross section is equal to

$$\sigma_{in} \;=\; \int d^2\, b_\perp \; G_{in}(s, b_\perp) \;=\; \int d^2 b_\perp \left(1 \;-\; e^{-\,\sigma(r_\perp, q^2_\perp = 0)\; S(b^2_\perp)} \right) . \tag{32}$$

We assume that the form of the final state is a uniform parton distribution that follows from the QCD evolution equations. Note that we neglect the contribution of all diffraction dissociation processes to the inelastic final state (in particular to the "fan" diagrams which give an important contribution[2]), as well as diffraction dissociation in the region of small masses[21], which cannot be presented as a decomposition of the $\bar{q}q$ wave function. We evaluate this input hypothesis in the next section.

In the language of Feynman diagrams, Eq.(32) sums all diagrams of Fig.3 in which the $\bar{q}q$ pair rescatters with the target, and exchanges "ladder" diagrams, each of which corresponds to the gluon density. This sum has already been performed by Mueller[9], and we will only comment on how one can obtain the result, without going into details.

The simplest way is to consider the inelastic cross section (see Refs.[2,9]), which has a straightforward interpretation through the parton wave function of the hadron (see Fig.4), as all partons are produced on the mass shell. In leading $\ln\frac{1}{x}$ approximation we have two orderings in time (see Fig.4):

1. The time of emission of each "ladder" by the fast $\bar{q}q$ pair, which should obey the obvious ordering for n produced "ladders"

$$t_1 \;>\; t_2 \;\ldots\; >\; t_i \;>\; t_{i+1} \;\ldots >\; t_n \, . \tag{33}$$

2. Each additional "ladder" which should live for a shorter time than the previous one. This gives a second ordering

$$t_1 - t'_1 \;>\; t_2 - t'_2 \;>\; \ldots \;>\; t_i - t'_i \;>\; \ldots \;>\; t_n - t'_n \, . \tag{34}$$

Each "ladder" in the leading log approximation has the same functional dependence on $t_i - t_i'$, which we denote as $\sigma(t-t', r_\perp^2)$. This fact allows us to carry out the integration over t_i and $t_i - t_i'$, which gives for n emitted cascades

$$\sigma_n \;=\; \frac{1}{(n!)^2}\int^{t} dt_1 \int^{t-t'} d(t_1 - t_1')\;\sigma^n(t_1 - t_1', r_\perp^2)\;. \tag{35}$$

For the case of the $\bar{q}q$ pair, both last integrations are not logarithmic, and in the LLA we can safely replace the above integral with

$$\sigma_n \;=\; \frac{1}{(n!)^2}\;\sigma^n(t-t', r_\perp^2)\;, \tag{36}$$

$t-t'$ is of the order of $\frac{1}{q_\parallel}$ due to the uncertainty principle, where $q_\parallel = \frac{Q^2+m_V^2}{s}$. One $n!$ is compensated by the number of possible diagrams, since the order of the "ladders" are not fixed. Therefore, the contribution of the nth "ladder" exchange gives

$$\sigma_n \;=\; \frac{1}{n!}\;\sigma^n(x, r_\perp^2)\;. \tag{37}$$

Applying the AGK cutting rules[22], we reconstruct the total cross section which results in Eq.(32).

3.2 Damping factor for diffractive production of vector meson

Substituting σ^{SC} of Eq.(32) in Eq.(9) and using σ in the form of Eq.(14) and the representation (17) for the wave function of the photon, we can easily estimate the general term of the expansion with respect to the power of σ. It has the form

$$M_f^n = C\int_0^1 dz\frac{Qz(1-z)}{2}\int_0^\infty \frac{dt}{t}\,exp\left(-\frac{1}{2}[t\;+\;\frac{a^2\,r_\perp^2}{t}\,]\right)\frac{(-1)^{n-1}}{n!}\left(\frac{\alpha_S\,4C_F\pi^2}{N_c^2-1}\right)^n \tag{38}$$

$$\prod_i^n \int_{C_i}\frac{d\omega_i}{2\pi i}\;g_i(\omega_i)\;\frac{\Gamma(1+\gamma(\omega_i))\;\Gamma(1-\gamma(\omega_i))}{(\Gamma(2-\gamma(\omega_i))^2}$$

$$\left(\frac{r_\perp^2}{4}\right)^{n\,-\,\sum_i^n\gamma(\omega_i)}\;[\Psi^V(r_\perp=0,z)]^*\;\int d^2b_\perp\;S^n(b_\perp^2)\;.$$

Taking the integrals over $r_\perp$, t and $b_\perp$ we obtain

$$M_f^n = C\;B'\int_0^1 dz\frac{Qz(1-z)}{2\,a^2}\;\frac{(-1)^{n-1}}{n\;n!}\left(\frac{\alpha_S\,C_F\pi}{B'(N_c^2-1)}\right)^n \tag{39}$$

$$\prod_i^n \int_{C_i}\frac{d\omega_i}{2\pi i}\;g_i(\omega_i)\;\frac{\Gamma(1+\gamma(\omega_i))\;\Gamma(1-\gamma(\omega_i))}{(\Gamma(2-\gamma(\omega_i))^2}$$

$$\Gamma^2(1+n-\sum_i^n \gamma(\omega_i))\ \left(\frac{4}{a^2}\right)^n\ (a^2)^{\sum\gamma(\omega_i)}\ [\Psi^V(r_\perp=0,z)]^*\ .$$

In the double log approximation of pQCD, $\gamma(\omega_i) \ll 1$ and we derive a very simple formula (neglecting γ). Taking the integral over ω_i we have

$$M_f^n = C\ B'\ \int_0^1 dz \frac{Qz(1-z)}{2a^2}\ \frac{(-1)^{n-1}n!}{n} \tag{40}$$

$$\left(\frac{C_F\pi}{B'(N_c^2-1)}\ \frac{4}{a^2}\ \alpha_S\ xG(a^2,x)\right)^n\ [\Psi^V(r_\perp=0,z)]^*\ .$$

Finally for M_f we have

$$M_f\ =\ C\ B'\ \sum_{n=1}^{\infty}\int_0^1 dz \frac{Qz(1-z)}{2a^2}\ (-1)^{n-1}(n-1)! \tag{41}$$

$$\left(\frac{C_F\pi}{B'(N_c^2-1)}\ \frac{4}{a^2}\ \alpha_S\ xG(a^2,x)\right)^n\ [\Psi^V(r_\perp=0,z)]^*\ .$$

The above series can be written in terms of the analytical function E_1 (see Ref.[19]), namely

$$M_f\ =\ C\ B'\ \int_0^1 dz \frac{Qz(1-z)}{2a^2}\ E_1(\frac{1}{\kappa})\, e^{\frac{1}{\kappa}}\ [\Psi^V(r_\perp=0,z)]^*\ , \tag{42}$$

where (for N_c= 3)

$$\kappa_q\ =\ \frac{2}{3}\cdot\frac{\alpha_S\pi}{B'\ a^2}\ xG(a^2,x)\ . \tag{43}$$

Using the above equation we have for the damping factor

$$D^2\ =\ \frac{\{\int_0^1 dz \frac{Qz(1-z)}{2a^2}\ E_1(\frac{1}{\kappa_q})\, e^{\frac{1}{\kappa_q}}\ \Psi^V(r_\perp=0,z)\}^2}{\{\int_0^1 dz \frac{Qz(1-z)}{2a^2}\ \kappa_q\ \Psi^V(r_\perp=0,z)\}^2}\ . \tag{44}$$

For the case of heavy mesons we can use the nonrelativistic approach $z \to \frac{1}{2}$, and the above formula has the very simple form

$$D^2\ =\ \frac{\{E_1(\frac{1}{\kappa_q})\, e^{\frac{1}{\kappa_q}}\}^2}{\kappa_q^2}\ . \tag{45}$$

The behaviour of the damping factor can be easily found using the well known property of E_1. Namely, at $\kappa_q \ll 1$, we have $D^2 \to 1$ while at $\kappa_q \gg 1$ the damping factor vanishes as $D^2 \propto \frac{\ln^2\kappa_q}{\kappa_q^2}$. The behaviour of the damping factor as a function of κ is given in Fig.5.

4 The relation between DIS diffractive production of vector mesons and $F_2(Q^2, x)$.

The expression for the F_2 structure function was derived by Mueller[9] and in our notation has the following form

$$\Sigma(Q^2, x) \;=\; \int_0^1 dz \int \frac{d^2 r_\perp}{2\pi}\; \Psi_\perp^{\gamma^*}(Q^2, r_\perp, z)\; \sigma^{SC}(r_\perp)\; [\Psi_\perp^{\gamma^*}(Q^2, r_\perp, z)]^* \;, \qquad (46)$$

where

$$\Sigma(Q^2, x) \;=\; \frac{F_2(Q^2, x)}{\langle e^2 \rangle} \;. \qquad (47)$$

$\langle e^2 \rangle$ denotes the average quark charge, which is equal to $\frac{2}{9}$ ($\frac{5}{18}$) for three (four) active flavors respectively.

$\Psi_\perp^{\gamma^*}$ represents the wave function of the virtual photon with transverse polarization. $\Psi_\perp^{\gamma^*}$, as needed for our calculations, has been given in Ref.[9] (see also Refs.[17,23]) i.e.

$$\Psi_\perp^{\gamma^*}(Q^2, r_\perp, z) \;=\; a\, K_1(a r_\perp) \;. \qquad (48)$$

However, as was shown in Ref.[9], within the LLA of pQCD, after integration over z in Eq.(46), we can safely replace this function by $\frac{1}{r_\perp^2}$. Finally Mueller's result reads (for $N_c = N_f = 3$) *

$$\Sigma(Q^2, x) \;=\; \frac{4}{\pi^2} \int \frac{d^2 b_\perp}{\pi} \int_{\frac{4}{Q^2}}^{\infty} \frac{d^2 r_\perp}{\pi}\; \frac{1}{r_\perp^4}\; \sigma^{SC}(r_\perp) \;. \qquad (49)$$

Comparing this equation with the general Eq.(9) we conclude that

$$M_f \;=\; \sqrt{N_f}\; \frac{4}{\pi^2} \int_0^1 dz \int_{\frac{4}{Q^2}}^{\infty} \frac{d^2 r_\perp}{\pi}\; [\Psi^V(r_\perp, z)]^*\; \frac{\partial \Sigma(\frac{4}{r_\perp^2}, x)}{\partial \ln \frac{1}{r_\perp^2}} \;. \qquad (50)$$

Using the notations of Ref.[7] and our normalization of the amplitude, we can rewrite the expression for the amplitude in the form

$$f(\gamma^* \to V) \;=\; \frac{4 e f_V}{\sqrt{2}} \int_0^1 dz\, Q\, z(1-z) \int_{\frac{4}{Q^2}}^{\infty} r_\perp^3\, dr_\perp\; K_0(a r_\perp) \qquad (51)$$

$$\frac{\partial F_2^{exp}(\frac{1}{r_\perp^2}, x)}{\partial \ln \frac{1}{r_\perp^2}}\; \frac{\frac{1}{2}\,\varphi^V(z)}{\int dz\, \varphi^V(z)} \;,$$

where $\varphi^V(z) \;=\; \Psi^V(r_\perp = 0, z)$.

*We thank A. Mueller for a discussion with us on this problem.

The atractive feature of the above formula is that it takes into account all shadowing corrections in the LLA of pQCD, and expresses the cross section for vector meson production directly through the experimental observable. We note that without SC this formula is trivial and follows directly from the GLAP evolution equations in the LLA of pQCD (see, for example, Ref.[24]). The shortcoming of this formula is obvious: we cannot perform the integration over $r_\perp$ as has been done in Eq.(44). We think that this formula will be especially useful for reactions with a nuclear target, since it absorbs all SC which are essential in this case.

Using Eq.(51) we can rewrite the expression for the damping factor in the form

$$D^2 \;=\; \frac{\{\int_0^1 dz\, Q\, z(1-z) \int r_\perp^3\, dr_\perp\, K_0(a\, r_\perp)\, \frac{\partial F_2^{exp}(\frac{1}{r_\perp^2},x)}{\partial \ln \frac{1}{r_\perp^2}}\, \frac{\frac{1}{2}\,\varphi^V(z)}{\int_0^1 dz\,\varphi^V(z)}\}^2}{\{\int_0^1 dz\, Q\, z(1-z) \int r_\perp^3\, dr_\perp\, K_0(a\, r_\perp)\, \frac{\partial F_2^{GLAP}(\frac{1}{r_\perp^2},x)}{\partial \ln \frac{1}{r_\perp^2}}\, \frac{\frac{1}{2}\,\varphi^V(z)}{\int dz\,\varphi^V(z)}\}^2}\,. \qquad (52)$$

In the case of a nuclear target, we have

$$\frac{\partial F_2^{GLAP}(A)}{\partial ln \frac{1}{r_\perp^2}} \;=\; A \frac{\partial F_2^{GLAP}(N)}{\partial ln \frac{1}{r_\perp^2}}\,,$$

where $F_2(N)$ is the structure function for a DIS with a nucleon. The last remark makes the whole expression of Eq.(52) useful for a nuclear target, since all values that enter the formula can be measured experimentally. In the case of a nucleon target, we have to rely on the solution of the GLAP evolution equations to estimate the denominator.

5 Shadowing corrections for the gluon distribution

To calculate the damping factor using Eq.(44) we need to calculate the SC for the gluon distribution. We anticipate that these shadowing correction will be large as

1. The cross section of the interaction of two gluons with a transverse separation $r_\perp$ is bigger than for $\bar{q}q$ pair and is equal to[9]

$$\sigma^{GG} \;=\; \frac{3\alpha_s}{4}\,\pi^2\, r_\perp^2\, xG(\frac{4}{r_\perp^2},x)\,. \qquad (53)$$

2. Each gluon in the parton cascade can interact with the target. Such interactions generate the so called "fan" diagrams (see Fig.6), which are essential in the region of small x, and correspond to the interaction of a fast GG pair[2] (see Fig.3).

In this paper we chose the following strategy of how to calculate the SC to the gluon distribution. First, we consider the SC for the fast gluon and discuss the contribution of the large distances. After that, we will discuss the contributions of the "fan" diagrams.

The SC for the fast GG pair has been calculated by Mueller[9], and in our notation the gluon distribution has the form ($N_c = N_f = 3$)

$$xG(Q^2,x) \;=\; \frac{4}{\pi^2}\int_x^1 \frac{dx'}{x'}\int \frac{d^2\,b_\perp}{\pi}\int_{\frac{4}{Q^2}}^{\infty}\frac{d^2\,r_\perp}{\pi}\,\frac{1}{r_\perp^4}\,2\{1\;-\;e^{-\frac{1}{2}\sigma^{GG}(r_\perp^2,x')\,S(b_1^2)}\}\;. \qquad (54)$$

To understand the physical meaning of this equation it is instructive to write down the evolution equation for the gluon density. Indeed,

$$\frac{\partial^2 xG(Q^2,x)}{\partial\ln(1/x)\,\partial\ln Q^2} \;= \qquad (55)$$

$$\frac{N_C\alpha_S}{\pi}\;x\,G^{GLAP}(Q^2,x)\;+\;\frac{1}{\pi^2}\sum_{k=1}\frac{(-1)^k}{kk!}\,\frac{1}{(B'Q^2)^{(k-1)}}\,\left(\frac{\pi C_A\alpha_S x G^{GLAP}(Q^2,x)}{2}\right)^{k+1}\;.$$

The first term corresponds to the usual GLAP equations, while the second one takes into account the SC. It should be stressed that the term with $k=1$ (if treated as an equation as in Ref.[9]), is the same term that appears in the nonlinear GLR equation which sums the "fan" diagrams[2]. This term has been calculated using quite a different technique[25,26]. The coefficient in front of the other terms, reflects the fact that all correlations between the gluons have been neglected, despite the fact that the gluons are uniformly distributed in the target disc with a radius $R^2 = B'$.

Mueller's formula is not a nonlinear equation, it is the analogue of the Glauber formula for the interaction with a nucleus, which gives us the possibility to calculate the shadowing corrections using the solution of the GLAP evolution equations. Hence, this formula should be used as an input to obtain the complete effect of the SC, for the more complicated evolution equations, such as GLR[2], or the generalized evolution equations[27].

Calculating the sequent iterations of Mueller's formula gives us a practical way to estimate the value of the SC from more complicated Feynman diagrams, that have to be taken into account (diagrams such as in Fig.3). Certainly, the iteration of Muller's formula is not the most efficient way to calculate the SC correction in the region of extremely small x, but, it gives a systematic way to estimate the value of the SC due to gluon screening and it could be a reliable procedure in the HERA kinematic region where x is not too small.

Making use of the explicit form of $S(b_\perp)$ (see Eq.(29)), we take the integral over $b_\perp$ and obtain

$$xG(Q^2,x) \;=\; \frac{2}{\pi^2}\int_x^1\frac{dx'}{x'}\int_{\frac{1}{Q^2}}^{\infty}\frac{d^2\,r'_\perp}{\pi}\,\frac{B'}{r'^4_\perp}\,\{C\;+\;\ln\kappa_G(x',r'^2_\perp)\;+\;,E_1(\kappa_G(x',r'^2_\perp)\;\}\;, \qquad (56)$$

where C is the Euler constant and E_1 is the exponential integral (see Ref.[19] **5.1.11**) and

$$\kappa_G(x',r'^2_\perp) \;=\; \frac{3\alpha_S\pi r'^2_\perp}{2B'}\;x'G^{GLAP}(\frac{1}{r'^2_\perp},x'))\;. \qquad (57)$$

In our numerical estimates which will be presented in the next section we use this formula to calculate the SC due to gluon screening. We also make the second iteration of Eq.(56) substituting the result of the first iteration back into Eq.(56) in place of xG^{GLAP}. In this way we take into account the first contribution of the "fan" diagrams (see Fig.7). We will discuss the result of these calculation in the next section.

6 Numerics and comparison with experiment

6.1 Vector meson production in DIS without SC

We show in Fig.8a the dependence of $\sigma(\gamma^* p \to Vp)$ on x with no SC for some typical values of Q^2.

As we have seen in section 2, the pQCD matrix element for DIS production of vector mesons is given as a convolution of $\Psi^{\gamma^*}(Q^2, r_\perp, z)$, $\Psi^V(r_\perp, z)$ and $\sigma(r_\perp, {q_\perp}^2)$ where we are able to calculate the above when both γ^* and V are longitudinally polarized. The specifications of Ψ^{γ^*}, Ψ^V and σ used in our calculations are as follow:

1. We use the commonly utilized form for Ψ^{γ^*}, e.g. our Eq.(10).

2. For Ψ^V we use the two forms which were also used in Ref.[7]. The asymptotic form[28] denoted AS and the form suggested by Chernyak and Zhitnitsky[29] denoted CZ. We note that Braun and Halperin[30] have cast some doubts on the CZ form and have suggested a modified wave function not that different from the AS form. The difference between our results with the AS and the CZ inputs, as seen in Fig.8a, defines a theoretical margin of error due to the ambiguity in our knowledge of Ψ^V. This should be compared later on with the margin of difference introduced due to the SC.

3. The $\bar{q}q$ cross section is given in the LLA utilizing xG^{GLAP}, e.g. our Eq.(15), with the GRV parameterization[31]. In our opinion GRV is suitable for our calculations as they chose a small scale and as such their result for small x are close to the LLA, enabling a reasonably consistent calculation.

A semiquantitative calculation of $\sigma(\gamma^* p \to \rho p)$ has been presented by Brodsky et.al.[7] and is compared to the low energy NMC data[32] at $x = 0.06$ and $Q^2 = 10\ GeV^2$. We note a difference between the approximation used in Ref.[7] and ours. When calculating the cross section shown in Fig.8a we take into account a z dependence of $\sigma(r_\perp, {q_\perp}^2)$ introduced after the $r_\perp$ integration. Brodsky et.al. neglect this z dependence and as a result their calculation with the AS or CZ wave functions have a fixed ratio of $(\frac{3}{5})^2$. The equivalent ratio in our calculation depends on x and Q^2 as can be seen in Fig.8a. Note that in our integration we have a cutoff $a^2 = Q^2 z > {Q_0}^2 = 0.4 GeV^2$. The relatively strong dependence of the above ratio on x and Q^2 shows that the LLA used to obtain Eq.(19) does not work too well in the kinematical domain under investigation. We shall return to this point in section 7. Regardless of the above, the calculation of Ref.[7] and ours at $x = 0.06$ and $Q^2 = 10 GeV^2$ are mutually compatible and are comparable to the NMC data[32].

6.2 Vector meson production in DIS with SC

Fig 8a should be compared with Fig 8b where we present our results for $\sigma(\gamma^* p \to \rho p)$ with SC as defined in section 3. Inspection of Fig.8 shows that the reduction of the cross

sections due to SC is bigger than the margin of theoretical error shown by the difference between the AS and CZ calculations of Fig.8a. As such SC are demonstrated to be an important ingredient of the pQCD calculation and should not be ignored. The comparison between the screened and non screened calculations of $\sigma(\gamma^* p \to \rho p)$ are further shown in Fig.9 as a function of Q^2 for c.m. energies of $\sqrt{s}$ = 50, 100 and 150 GeV. As expected, the difference between the screened and non screened results gets smaller when Q^2 is increased and becomes bigger when $\sqrt{s}$ is increased.

Recently, some ZEUS data on $\sigma(\gamma^* p \to \rho p)$ became available[33], and when combined with the low energy NMC data[32] provide a first qualitative examination of the pQCD results.

1. The ZEUS differential cross section slope is found to be $B = 5.1 + 1.2 - 0.9 \pm 1.0 GeV^{-2}$. This B value is about a half of the slope found in elastic ρ^0 photoproduction and is in excellent agreement with our input[13,21].

2. ZEUS reports a Q^{-n} dependence of $\sigma(\gamma^* p \to \rho p)$ where $n = 4.2 \pm 0.8 + 1.4 - 0.5$. This should be compared with the (asymptotic) prediction of Brodsky et.al.[7] of n = 6. In our calculations n is a function of x and Q^2 approaching n = 6 when the SC are diminished. Note that $n \to 2$ when $ln\frac{1}{x}$ is big enough, actually well above the presently available HERA kinematics. In the low Q^2 domain investigated by ZEUS, $7 \leq Q^2 \leq 25 GeV^2$, our calculations result in n = 5.3 for AS and n = 4.8 for CZ. Clearly the present experimental errors are too big for a definite conclusion. Note, also, that the ZEUS results are obtained for $\sigma = \sigma_L + \sigma_T$ with $R = \frac{\sigma_L}{\sigma_T} = 1.5 + 2.8 - 0.6$, whereas the pQCD analysis applies to σ_L only.

3. The dependence of the ZEUS-NMC cross sections on x is compared with the pQCD results in Fig 10 for $x \leq 0.01$. The unscreened results calculated by ZEUS according to Ref.[7] are given by the shaded area, whereas the screened results are given by the two solid lines denoted CZ and AS. At this time the experimental errors are sufficiently large so as to accommodate both the screened and unscreened options. However, it is encouraging to note that a luminosity increase by a factor of 2-3 will enable a data based discrimination between the theoretical models. Note that the theoretical predictions on Fig.10 are obtained after a multiplication by R = 1.5, to account for the observed σ_T as well.

Fig.11 shows the contours of the damping factor D^2 (defined in Eq.(1) and evaluated in Eqs.(44,45)) as a function of $\sqrt{s}$ and Q^2 for $\gamma^* p \to J/\psi p$. Note that for heavy quarks the dependence on Ψ^V is eliminated in the nonrelativistic limit. Indeed, the difference between the AS and CZ results was small enough to be neglected. Experimental data on this reaction in the HERA energy range is now available[34] with $Q^2 \leq 4 GeV^2$. This data together with lower energy data is shown in Fig.12 together with some theoretical predictions. The shaded area corresponds to Ryskin's pQCD calculations[5] and our corrections to Ryskin's predictions are presented by the two solid lines. Note that ours is an approximate assessment due to the following uncertainties:

1. Ryskin uses the BFKL kernel whereas we use a GLAP kernel.

2. The shaded area in Fig.11 corresponds to the ZEUS experimental values for $xG(x,Q^2)$ inserted into Ryskin's calculations. Our calculation of D^2 is based on the GRV parameterization[31].

3. Ryskin uses a non relativistic quark model wave function for the vector meson, whereas we assume the relativistic wave functions which were also used in Ref[7]. This difference results in a normalization ambiguity between the two approximations which has not as yet been resolved.

Regardless of the above, an inspection of Figs.11 and 12 shows that if a pQCD calculation, with no SC, yields an energy dependence of $s^{2\Delta}$ for $\sigma(\gamma^* p \to J/\psi p)$, the imposition of SC will reduce Δ by approximately 0.08 for the Q^2 range of Ref.[34]. For real photoproduction, $Q^2 = 0$, the reduction in Δ will be 0.11.

6.3 The damping factor with SC for the gluon distribution

Fig.13 shows the damping factor for J/ψ production calculated using Eq.(56) for the gluon distribution and Eq.(9) for the vector production amplitude. As has been discussed, we anticipate a bigger influence of the small distances in the gluon damping than we have observed in the the quark sector with SC. The damping factor in the gluon sector is calculated to be

$$D_G^2 \;=\; \{\; \frac{xG(a^2(z=\frac{1}{2}),x)^{[Eq.(56)]} + xG^{GRV}(Q_0^2,x)}{\frac{N_c\alpha_S}{\pi}\int_x^1 \frac{dx'}{x'}\int_{Q_0^2}^{a^2}\frac{dQ'^2}{Q'^2}\,x'G^{GRV}(Q'^2,x') \;+\; xG^{GRV}(Q_0^2,x)} \;\}^2 \;, \qquad (58)$$

where $Q_0^2 = 0.4\ GeV^2$. This should be compared with Eq.(44) in the quark sector. In Eq.(56) we have integrated over $r_\perp^2$ from $\frac{1}{a^2}$ to $\frac{1}{Q_0^2}$. Note that the denominator of Eq.(56)is the Born Approximation of the numerator.Since we have seen that the LLA for the GLAP evolution equation does not work well in the kinematic region of interest, we also use this approximation for the denominator in our calculation as the SC is known only in LLA. We also demand that the initial condition for the gluon distribution is the same for SC and without them. Our reasoning is that we look on the initial condition as if it has been taken from the experiment. Therefore, the result of the calculation can be read in the following way: the suppression of J/ψ production is given by D_G^2 due to the screening at distances of $\frac{1}{Q_0^2} > r_\perp^2 > \frac{4}{Q^2}$. One can extract from Figs.12 and 13 that the SC corrections in the gluon sector, are as large as in the quark sector. This fact could be anticipated because the κ_G is $\frac{9}{4}$ times bigger than κ_q. Additional integration over x in Eq.(56) suppresses the gluon screening, but not to an extent that will make it smaller than SC in the quark sector.

The ratio $R = \frac{D_G^2(\ second\ \ iteration\ )}{D_G^2(\ first\ \ iteration\ )}$ is shown in Fig.14. R is the quantitative measure of the correction to the damping factor due to the second iteration of Eq.(56) which takes

into account the first correction from the "fan" diagrams (see Fig.7). One can see that this correction is rather big and we plan to study them in a more comprehensive way in a future publication.

7 Conclusions

1. The formulae for shadowing corrections for vector meson production in DIS have been obtained whihin the framework of the GLAP evolution equations in the low x region. It is shown that the rescattering of the quark is concentrated at small distances ($r_\perp \propto \frac{1}{a^2}$) and can be treated theoretically on the basis of pQCD. On the other hand, the rescattering of gluons depends on a wider range of the distances, including the larger ones where ($r_\perp > \frac{1}{a^2}$). This causes a large uncertainty in the pQCD calculations. We show that the gluon shadowing generates a damping factor which is compatible or bigger than the damping in the quark sector.

2.The numerical calculations of the differential cross sections for vector meson production has been performed using two models for the hadron wave function at small transverse distances. The results of the calculations show that the corrections due to the SC are bigger than the non screened uncertainties. There are two sources for these uncertainties: (i) the different nonperturbative models for Ψ^V at $r_\perp \to 0$ which, at the moment, are not under full theoretical control. And, (ii) the limited accuracy of the LLA for the GLAP equation in the available kinematic region. Basically, those uncertainties can be seen without a detailed calculation just by changing the scale of Q^2 (let say, from Q^2 to $Q^2/2$). However, we think that the exact integration over z in Eq.(9) has a certain meaning, since the GRV gluon structure function reaches the value of the anomalous dimension $\gamma = 1/2$ at $x \simeq 10^{-2}$. It means that at low values of x we can try to calculate the gluon distribution using the BFKL equation which has a well defined scale in Q^2. Therefore, the difference in the results due to the integration over z, allows us to estimate the theoretical uncertainties that originate from our poor knowledge of the nonperturbative wave function of the produced vector mesons.

3.The numerical calculation of the SC shows that (i) they should be taken into account in the HERA kinematic region, (ii) their value is bigger than the uncertainties related to the unknown nonperturbative part of our calculation, and (iii) DIS vector meson production can be used as a laboratory for the investigation of SC. In our opinion, using these reactions to extract the nonperturbative wave function of the produced vector mesons is all too ambiguous, at least with the present theoretical knowledge of SC.

4. The calculation of the SC for the gluon distribution has an intrinsic uncertainty, related to the large distance contribution. However, we wish to mention that the anomalous dimension in the GRV gluon distribution becomes larger than 1 ($\gamma > 1$) at $x < 10^{-3}$. It means that at such small x, all uncertainties from the large distance behaviour become rather small, especially at $a^2 \leq 2GeV^2$ (which corresponds to $Q^2 \leq 10GeV^2$ for the case of ρ production and $Q^2 \leq 4GeV^2$ for J/ψ production). We demonstrated that the

poor accuracy of our calculation in this kinematic region is due to the fact that the LLA for the GLAP equation is seriously ill in the HERA region. Much more work is needed to provide a reliable calculation of the shadowing corrections for the gluon distribution. We established the fact that the Mueller (Glauber - like) formula for the gluon SC cannot provide a reliable result as the second iteration of this formula gives a rather big correction. We propose to use this formula as an initial condition to solve the new evolution equations in the region of small x and we will publish a more detail study of this problem in the future.

5) The relationship between $\frac{\partial F_2^{exp}(Q^2,x)}{\partial\, ln Q^2}$ and the screened cross section for virtual photoproduction of vector mesons has been established. The relation includes all shadowing corrections and in our oppinion is suitable to extract the information on the non perturbative light cone $\bar{q}q$ vector meson wave function. To do this, we need to know $F_2^{exp}(Q^2, x)$ over a wide region of x and Q^2. With the appearance of the new HERA data we hope, that this will be possible in the very near future.

Figure Captions

Fig.1: Vector meson production in DIS without SC.

Fig.2: Extra gluon emission for vector meson production in DIS without SC.

Fig.3: SC for vector meson production in DIS.

Fig.4: The time structure of the SC in the inelastic cut of the diagram of Fig.3.

Fig.5: The behaviour of the damping factor D^2 versus $x = \kappa_q$ for J/ψ diffractive production.

Fig.6: "Fan" diagrams with triple "ladder" vertices γ.

Fig.7: The first iteration of the "fan" diagrams in the gluon distribution for vector meson leptoproduction.

Fig.8: The x dependence of $\sigma(\gamma^* p \to \rho p)$ with $Q^2 = 4, 9, 15, 20\ GeV^2$. a) In a pQCD calculation with no SC. b) In a pQCD calculation with SC. Solid lines correspond to a CZ wave function input and dashed lines to AS.

Fig.9: Comparison of screened (solid line) and nonscreened (dashed lines) calculated values of $\sigma(\gamma^* p \to \rho p)$ for $\sqrt{s} = 50, 100, 150\ GeV^2$. a) With AS input. b) With CZ input.

Fig.10: $\sigma(\gamma^* p \to \rho p)$ as a function of x at $Q^2 = 8.8$ and $16.9\ GeV^2$ taken from Ref.[33]. Shaded area corresponds to a pQCD calculation with ZEUS gluon densities and no SC. Solid lines are our AS CZ predictions in a pQCD calculation with SC.

Fig.11: A mapping of D^2 as a function of $\sqrt{s}$ and Q^2 for J/ψ electroproduction.

Fig.12: A compilation of $\sigma(\gamma p \to J/\psi p)$ taken from Ref.[34]. The solid line is a VDM prediction. The shaded area is the prediction of Ryskin[5] with ZEUS gluon densities. The dashed lines are our corrections to Ryskin's calculation.

Fig.13: The damping factor D_G^2 for J/ψ production due to first iteration screening in the gluon distribution for different values of a^2.

Fig.14: The ratio $R^2 = D_G^2(second\ iteration)/D_G^2(first\ iteration)$ for J/ψ production due to screening in the gluon distribution.

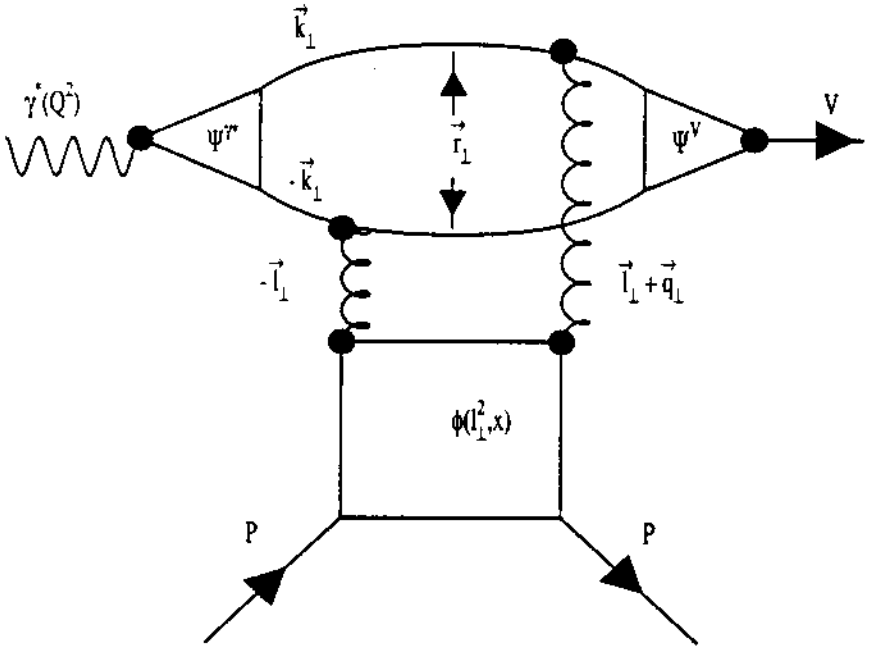

Figure 1: Vector meson production in DIS without SC.

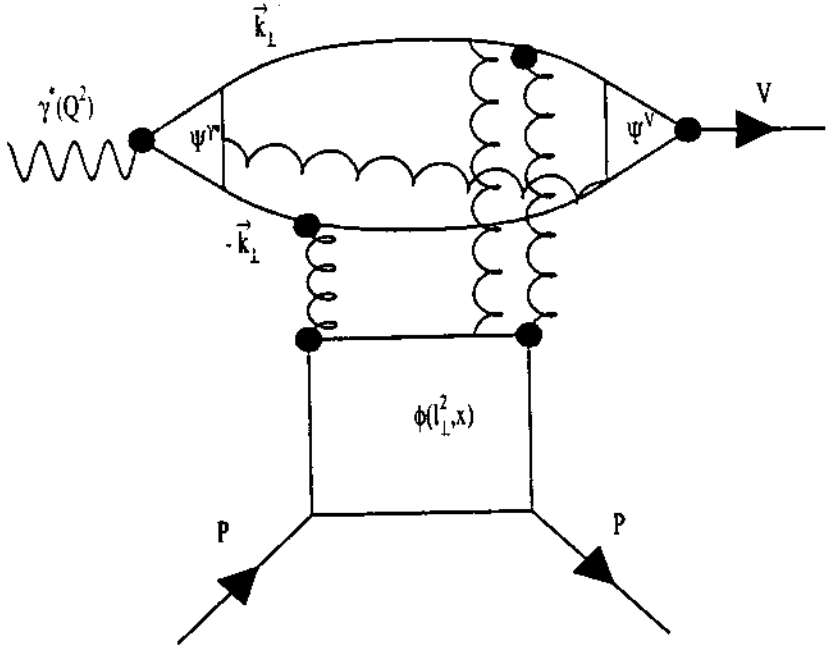

Figure 2: Extra gluon emission for vector meson production in DIS without SC.

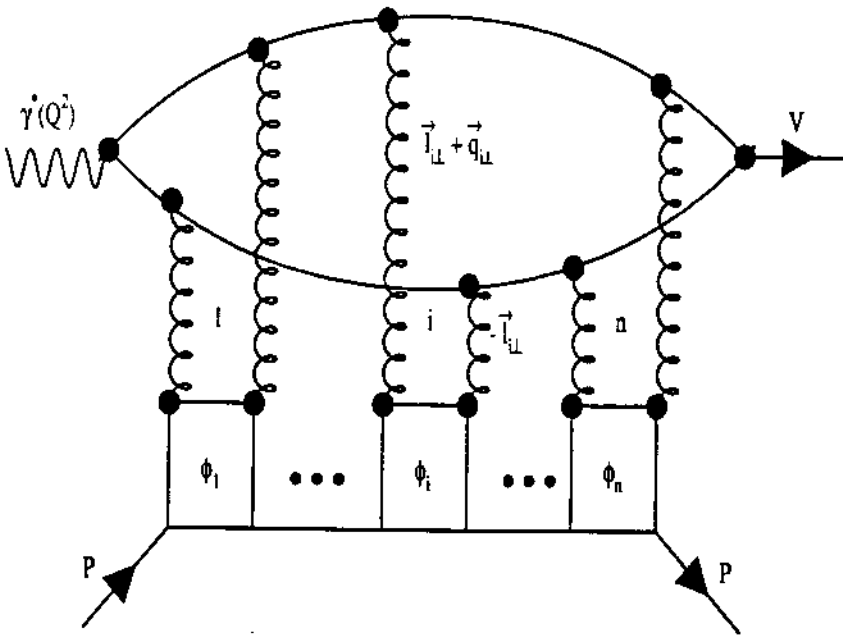

Figure 3: SC for vector meson production in DIS.

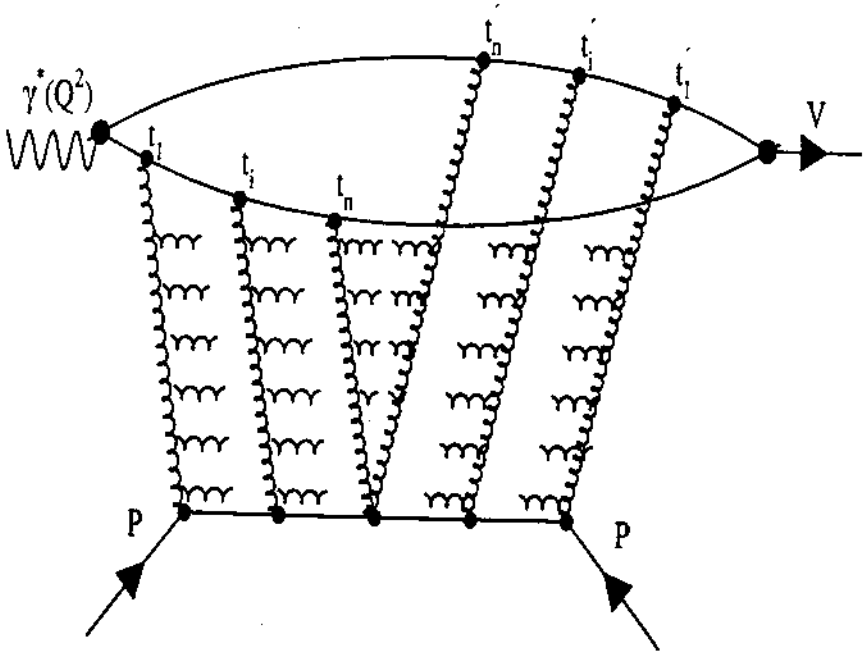

Figure 4: The time structure of the SC in the inelastic cut of the diagram of Fig.3.

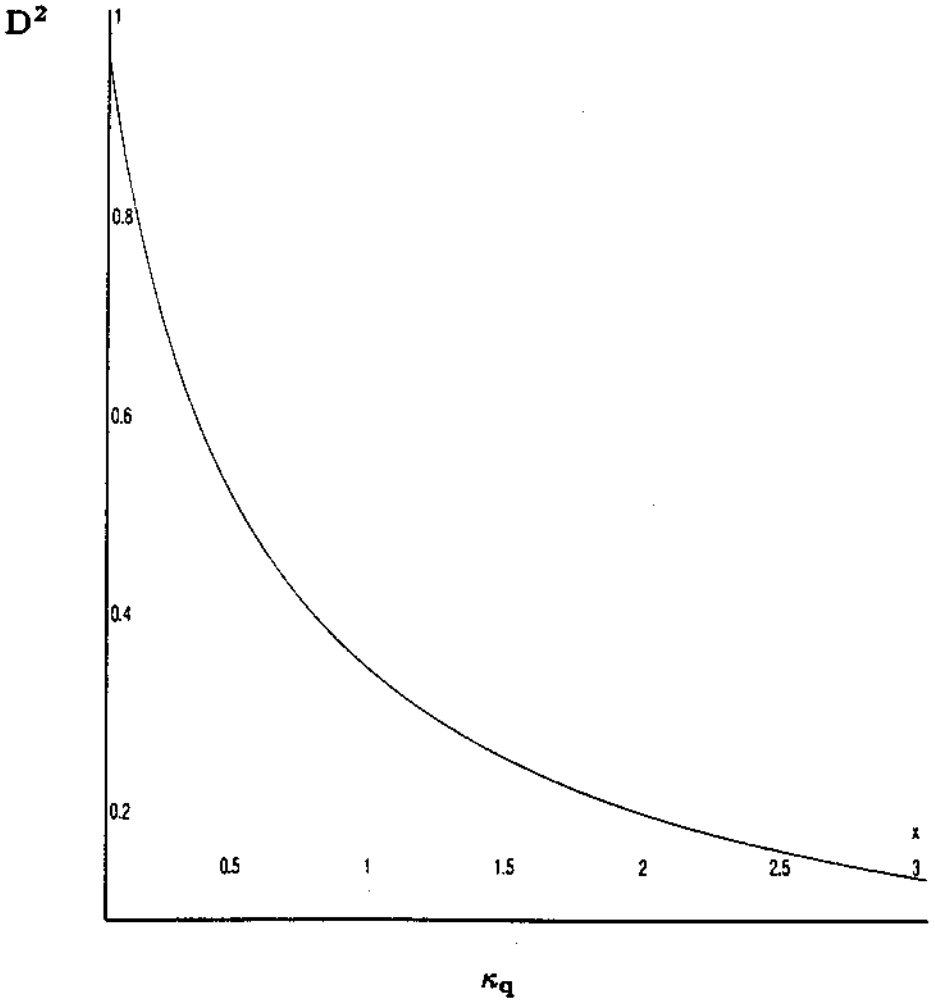

Figure 5: The behaviour of the damping factor D^2 versus $x = \kappa_q$ for J/ψ diffractive production.

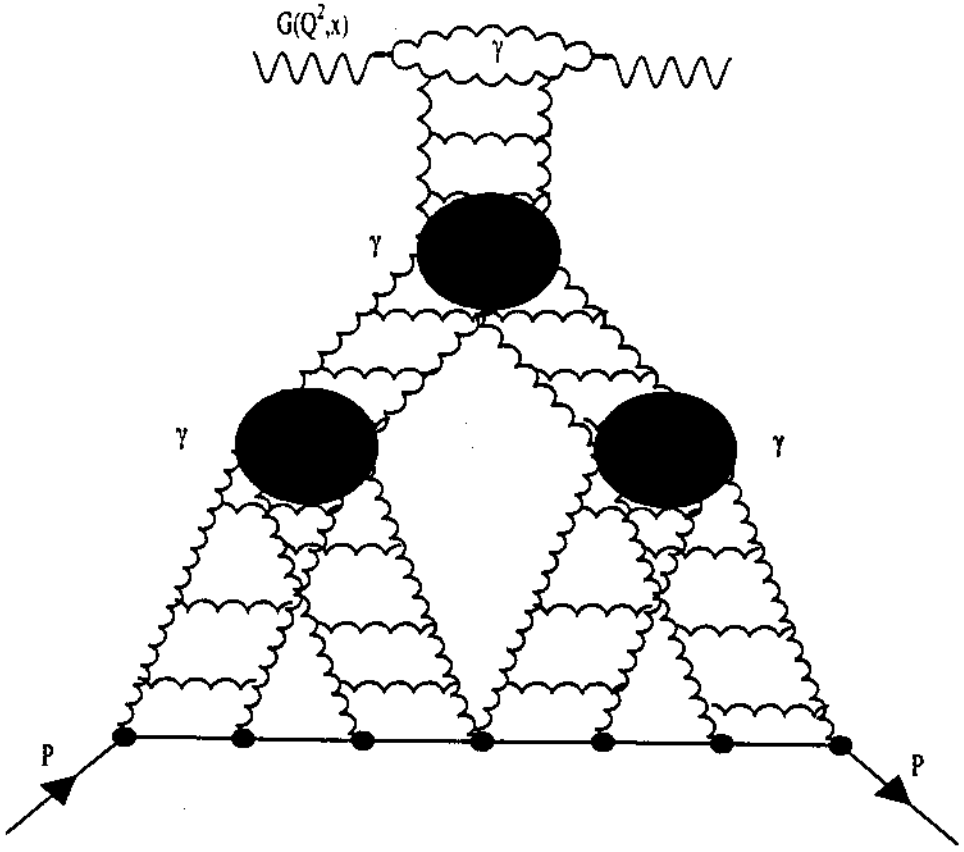

Figure 6: "Fan" diagrams with a triple "ladder" vertex.

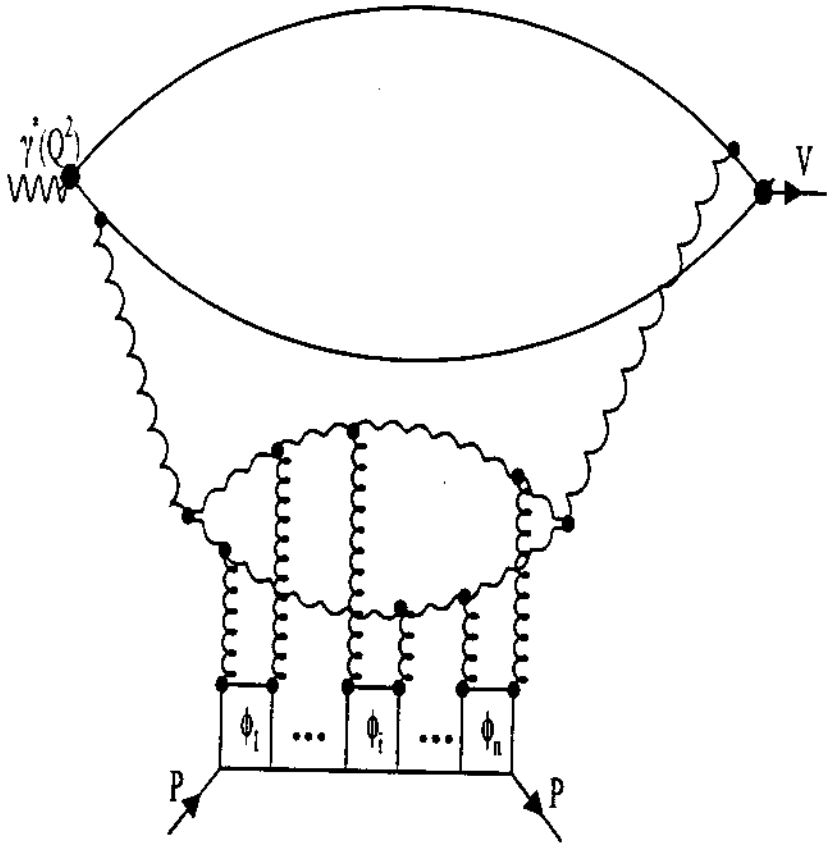

Figure 7: The first iteration of the "fan" diagrams in the gluon distribution for vector meson leptoproduction.

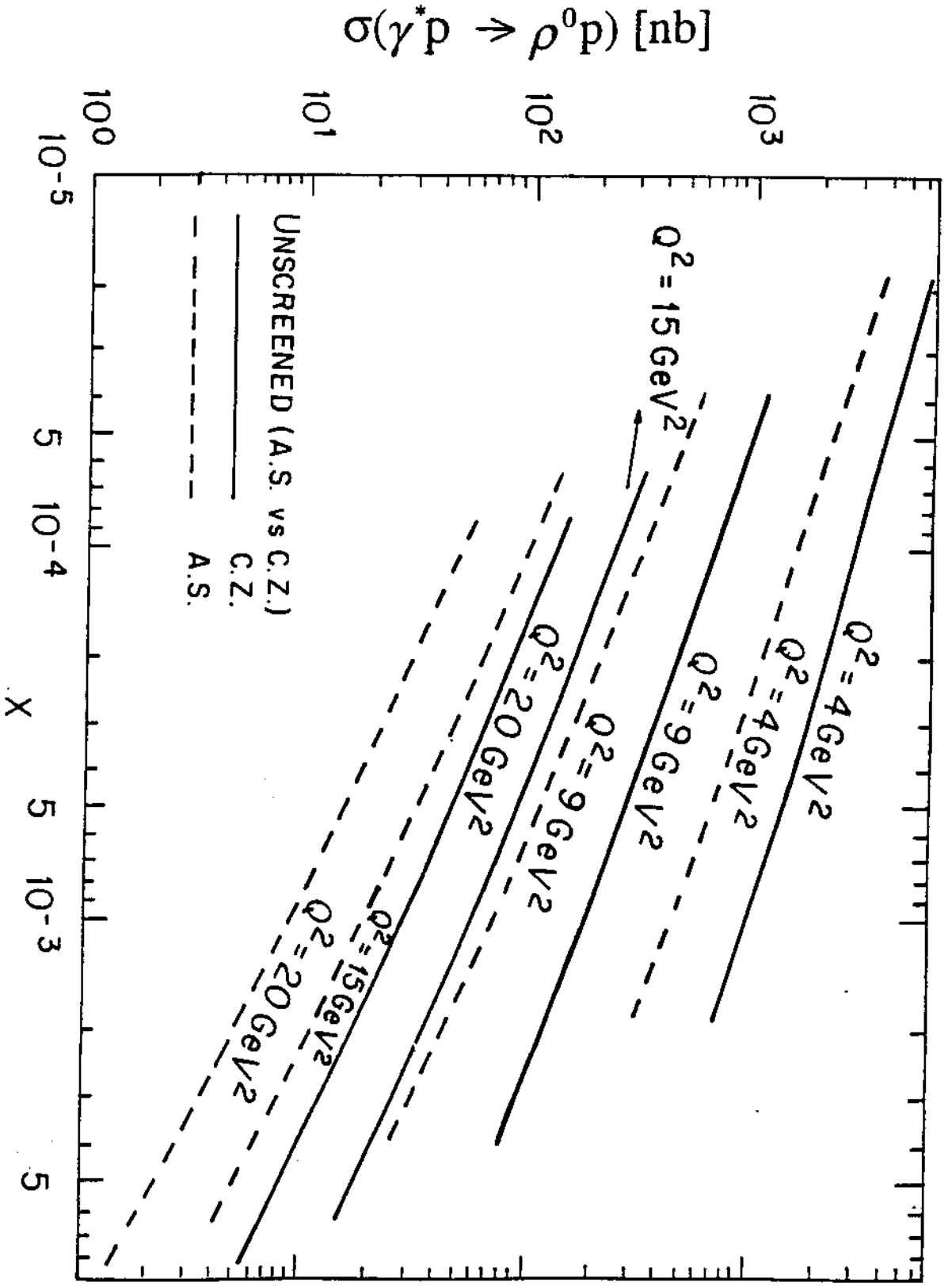
$\sigma(\gamma^* p \rightarrow \rho^0 p)$ [nb]
10^0
10^1
10^2
10^3
10^{-5}
5
10^{-4}
5
10^{-3}
5
X
UNSCREENED (A.S. vs C.Z.)
C.Z.
A.S.
$Q^2 = 15\ GeV^2$
$Q^2 = 4\ GeV^2$
$Q^2 = 9\ GeV^2$
$Q^2 = 20\ GeV^2$
$Q^2 = 15\ GeV^2$
$Q^2 = 4\ GeV^2$
$Q^2 = 9\ GeV^2$
$Q^2 = 20\ GeV^2$

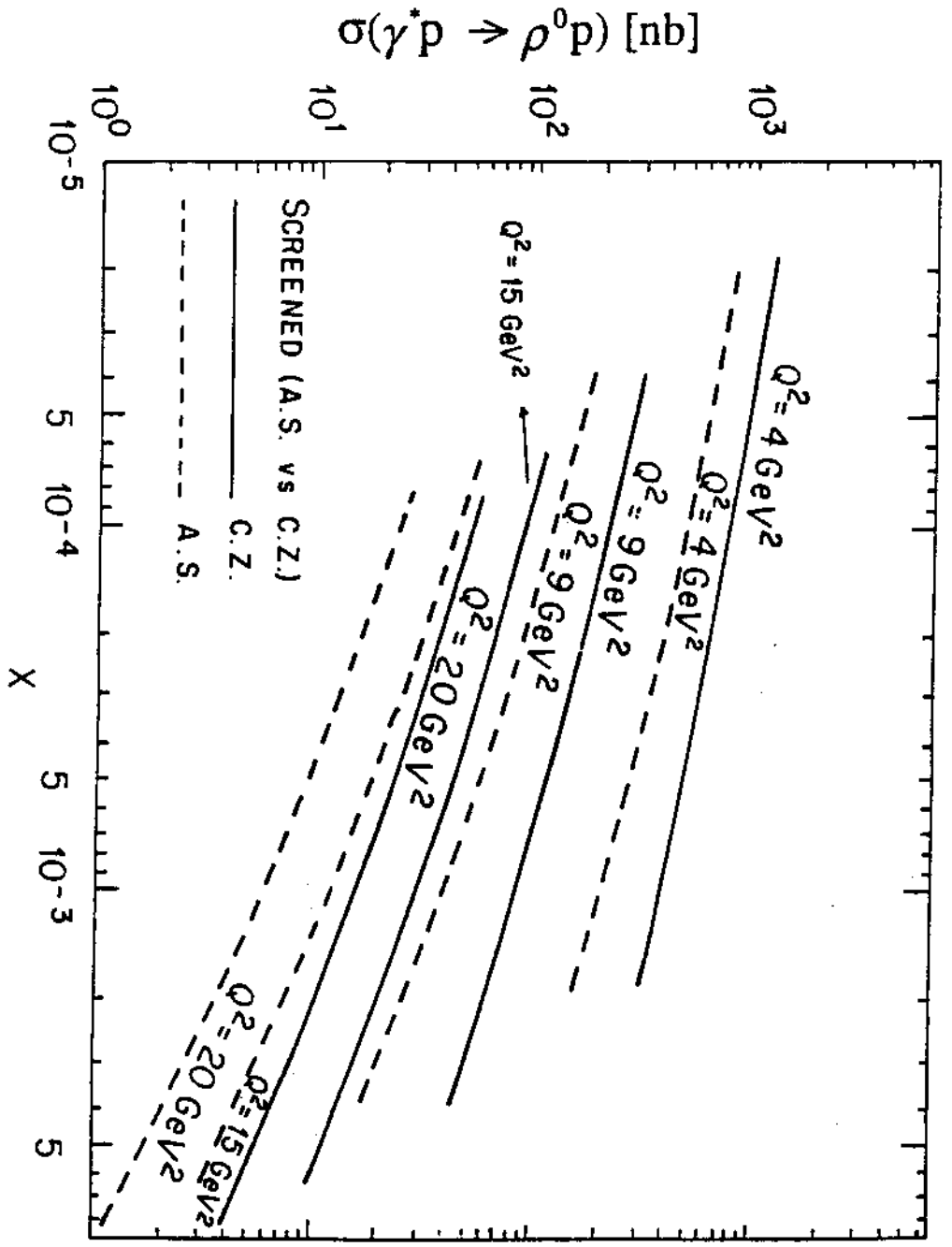

Figure 8: The x dependence of $\sigma(\gamma^* p \to \rho p)$ with $Q^2 = 4$, 9, 15, 20 GeV^2. a) In a pQCD calculation with no SC. b) In a pQCD calculation with SC. Solid lines correspond to a CZ wave function input and dashed lines to AS.

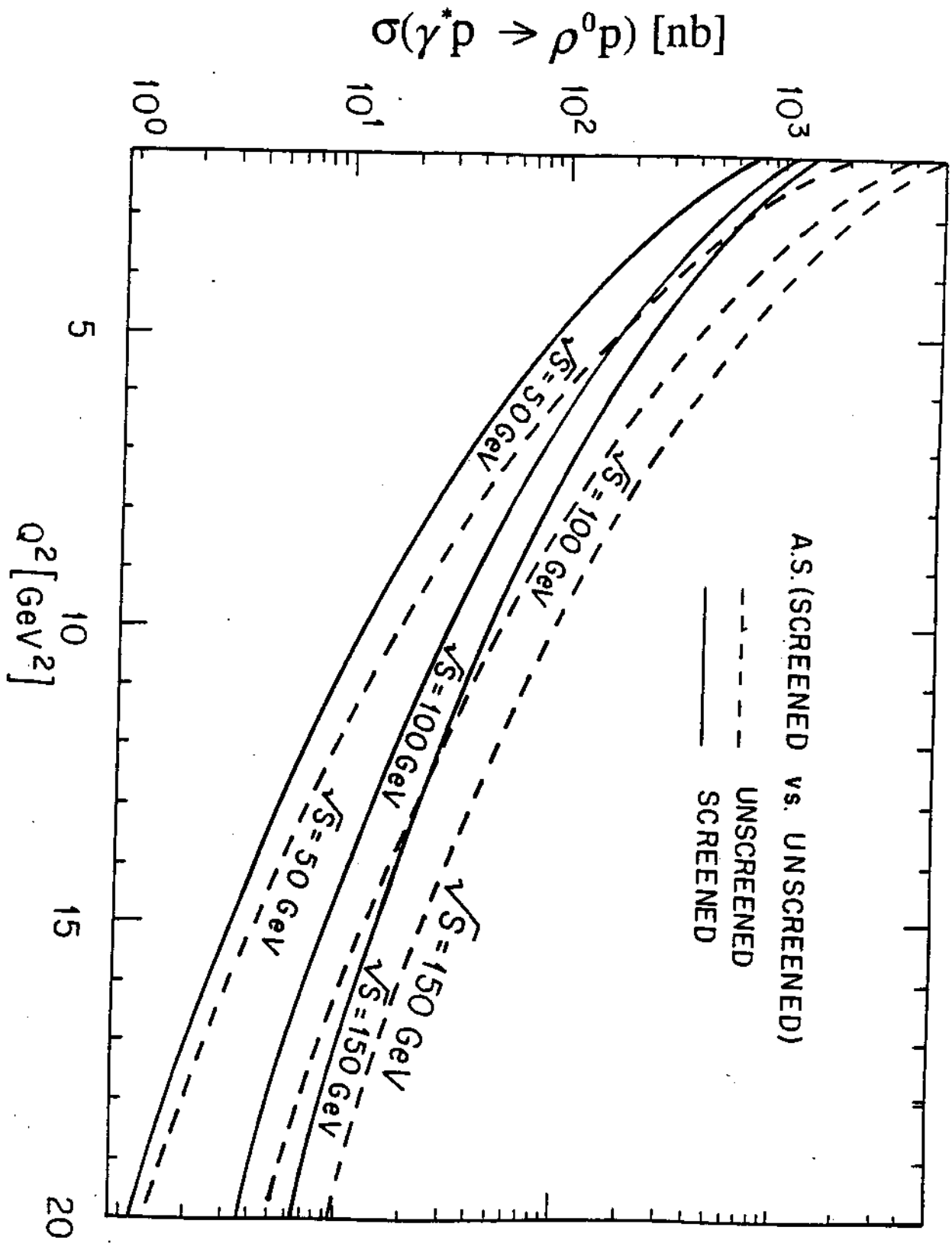
$\sigma(\gamma^* p \rightarrow \rho^0 p)$ [nb]
10^0
10^1
10^2
10^3
5
10
15
20
Q^2 [GeV^2]
A.S. (SCREENED vs. UNSCREENED)
UNSCREENED
SCREENED
$\sqrt{s}$= 50 GeV
$\sqrt{s}$= 100 GeV
$\sqrt{s}$= 150 GeV
$\sqrt{s}$= 50 GeV
$\sqrt{s}$= 100 GeV
$\sqrt{s}$= 150 GeV

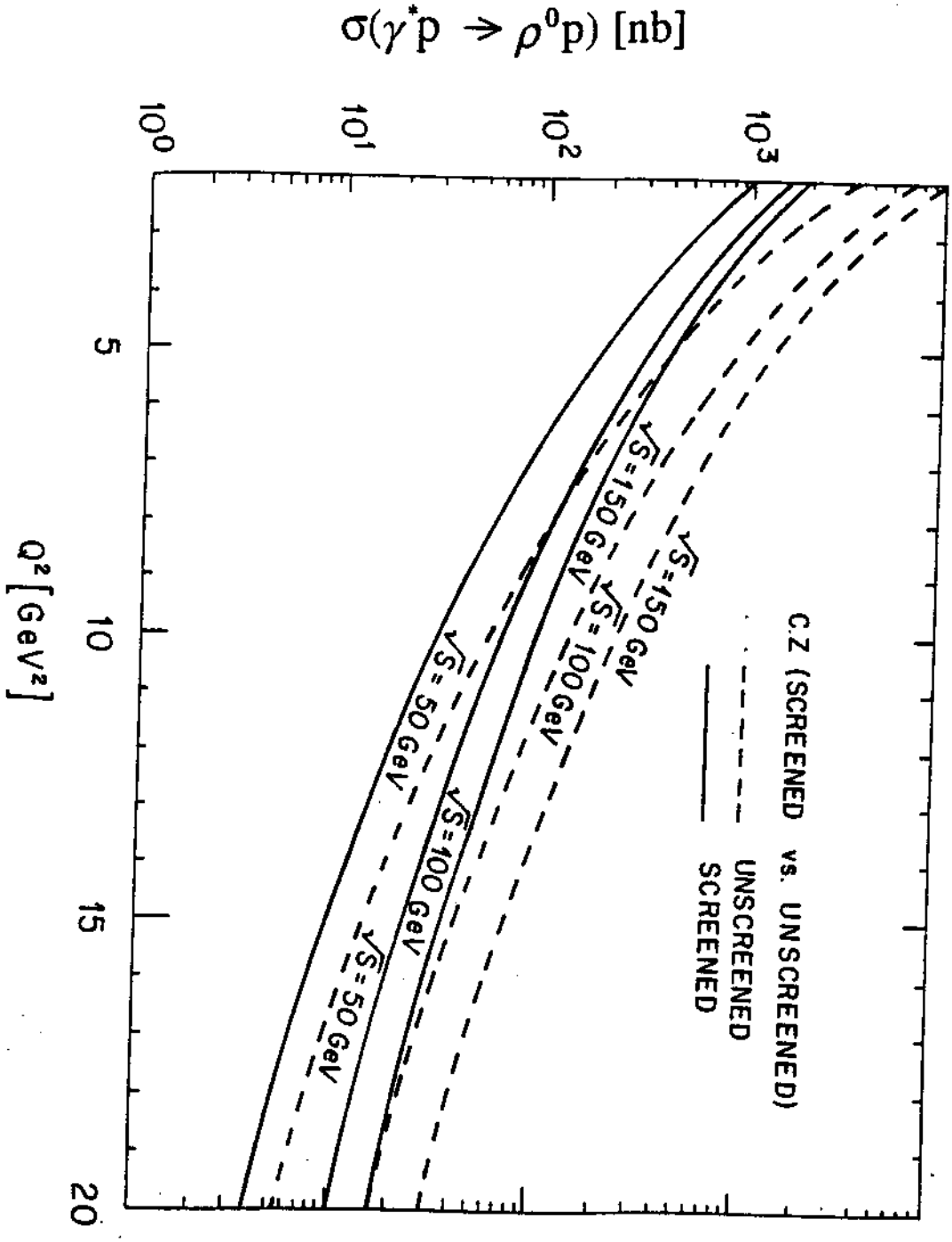

Figure 9: Comparison of screened (solid line) and nonscreened (dashed lines) calculated values of $\sigma(\gamma^* p \to \rho p)$ for c.m.energy of 50, 100, 150 GeV. a) With AS input. b) With CZ input.

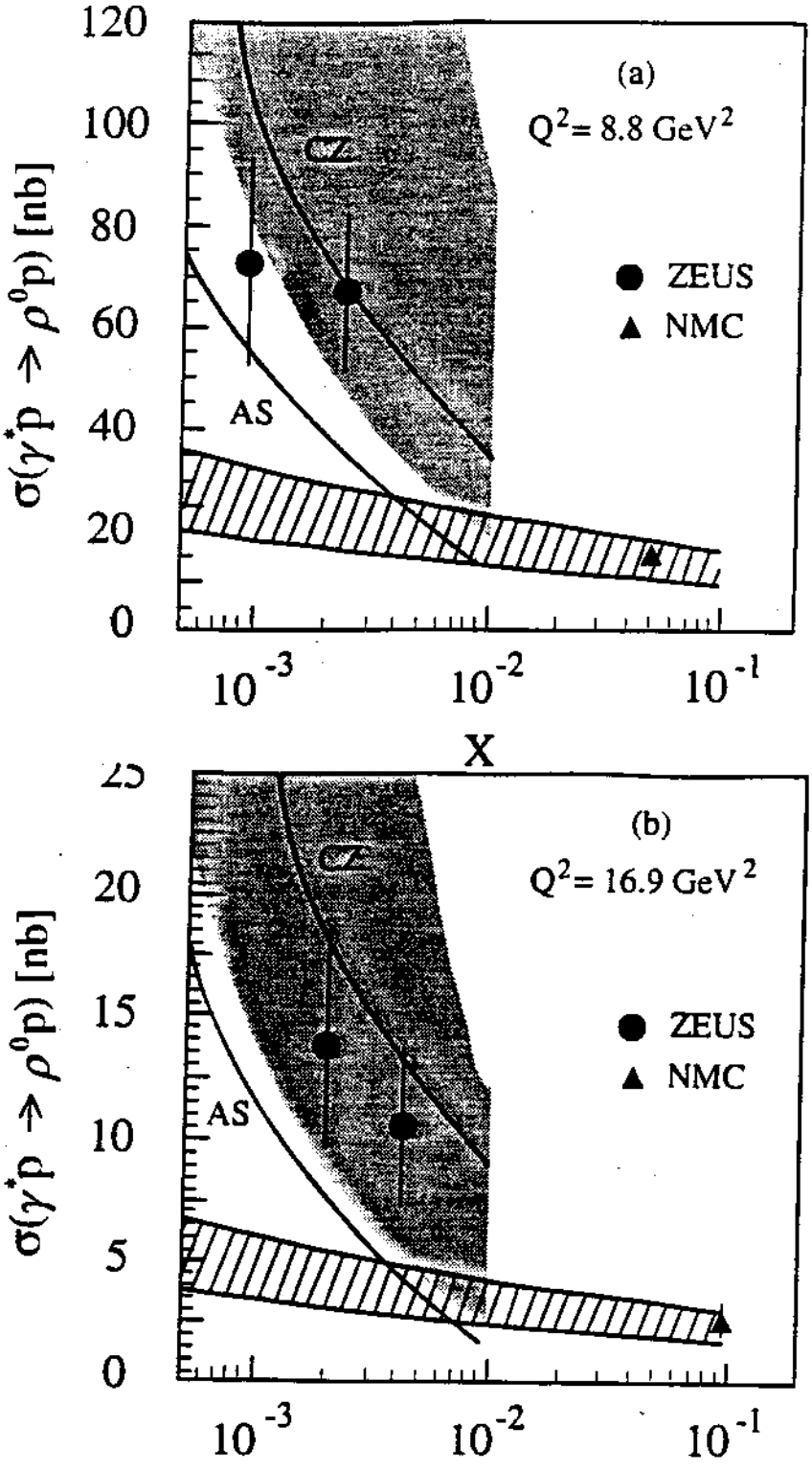

Figure 10: $\sigma(\gamma^* p \to \rho p)$ as a function of x at $Q^2 = 8.8$ and 16.9 GeV^2 taken from Ref.[33]. Shaded area corresponds to a pQCD calculation with ZEUS gluon densities and no SC. Solid lines are our AS CZ predictions in a pQCD calculation with SC.

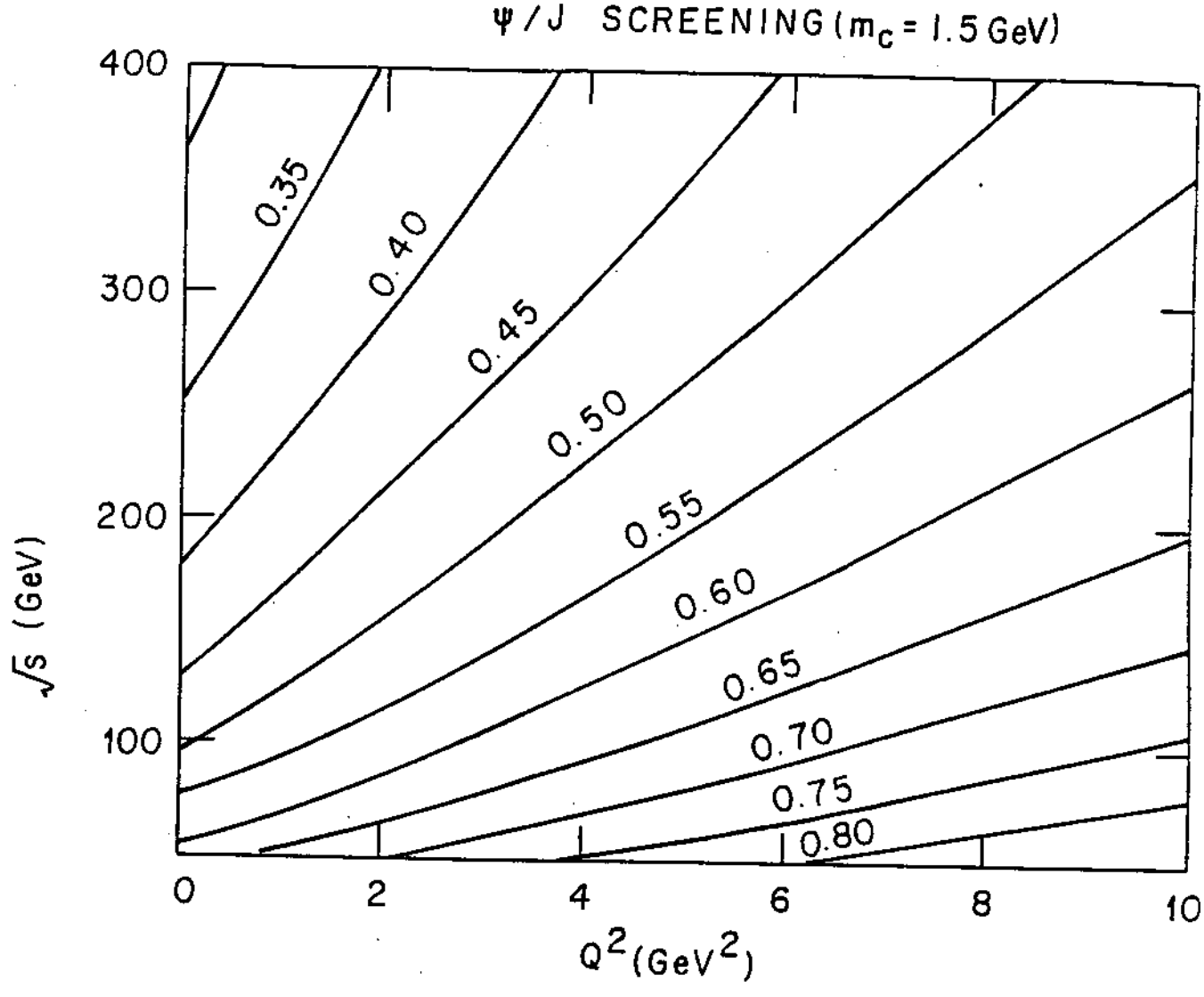

Figure 11: A mapping of D^2 as a function of c.m. energy and Q^2 for J/ψ electroproduction.

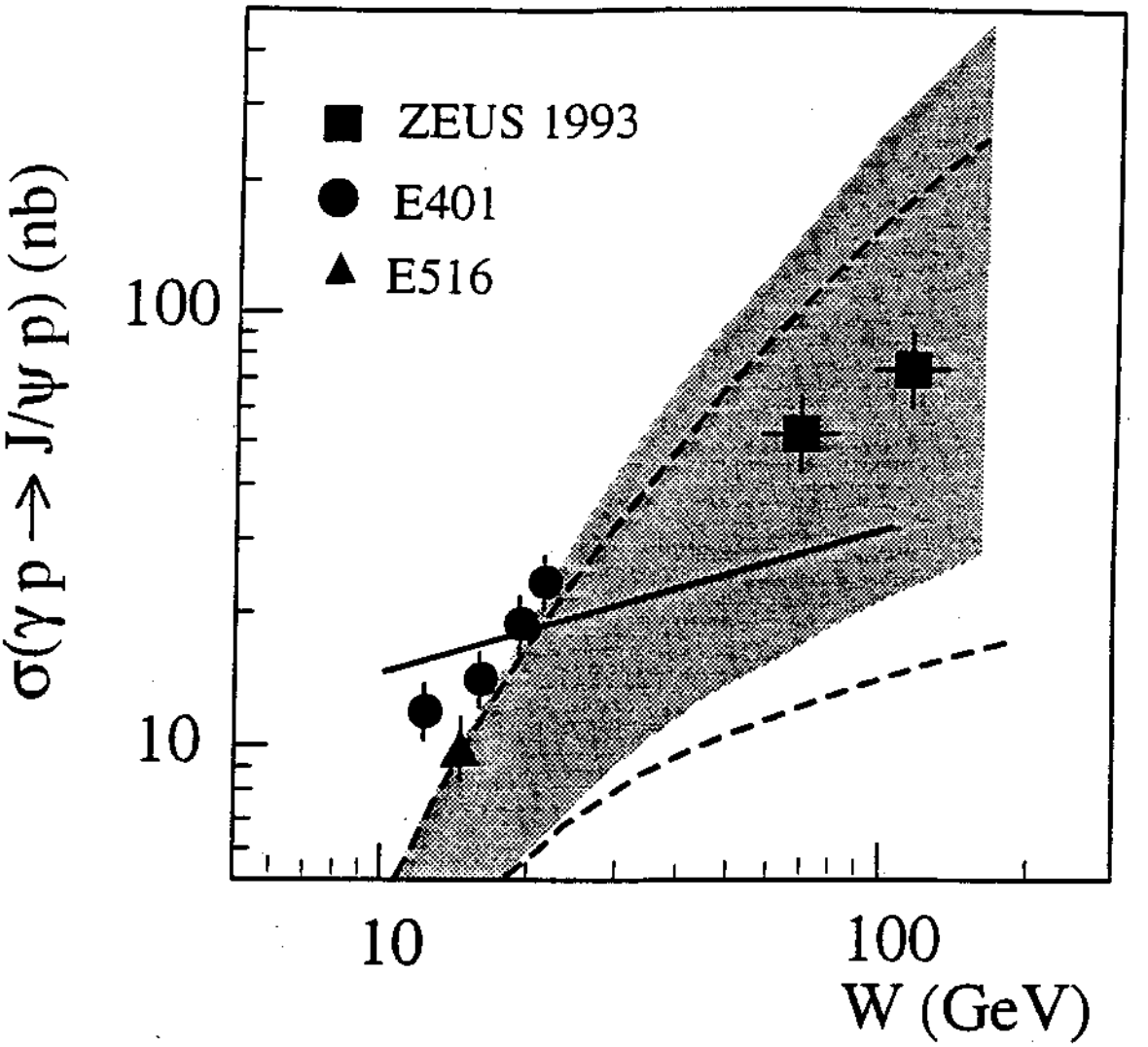

Figure 12: A compilation of $\sigma(\gamma p \to J/\psi p)$ taken from Ref.[34]. The solid line is a VDM prediction. The shaded area is the prediction of Ryskin[5] with ZEUS gluon densities. The dashed lines are our corrections to Ryskin's calculation.

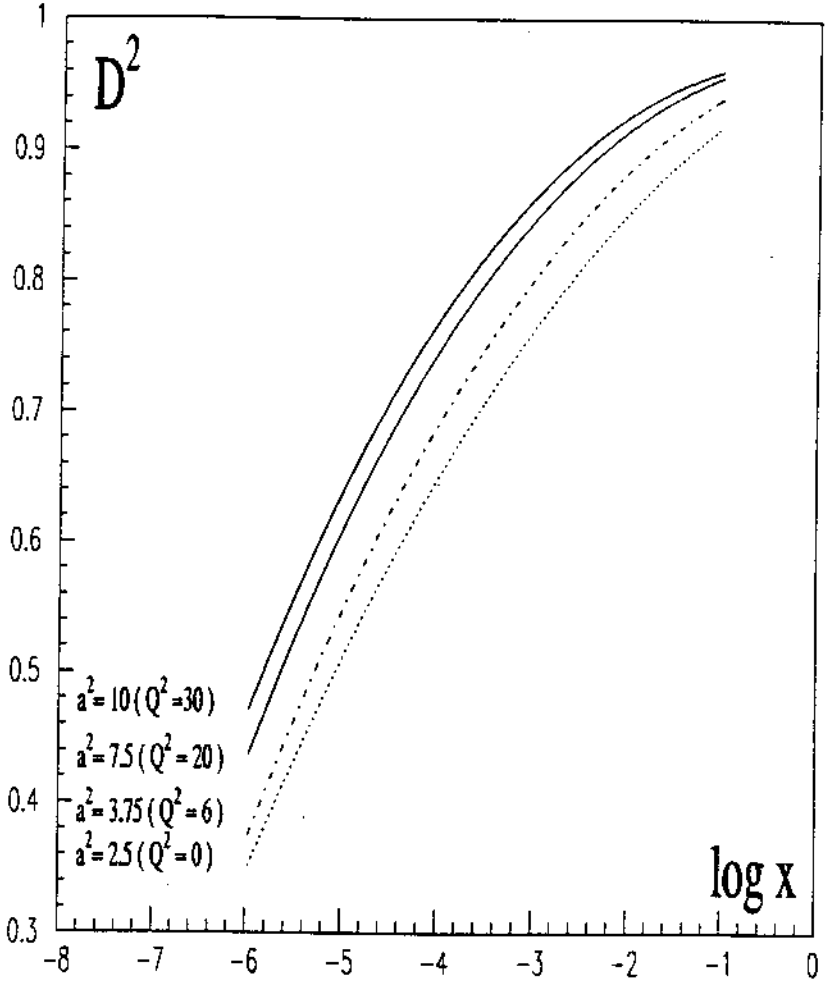

Figure 13: The damping factor D_G^2 for J/ψ production due to first iteration screening in the gluon distribution for different values of a^2.

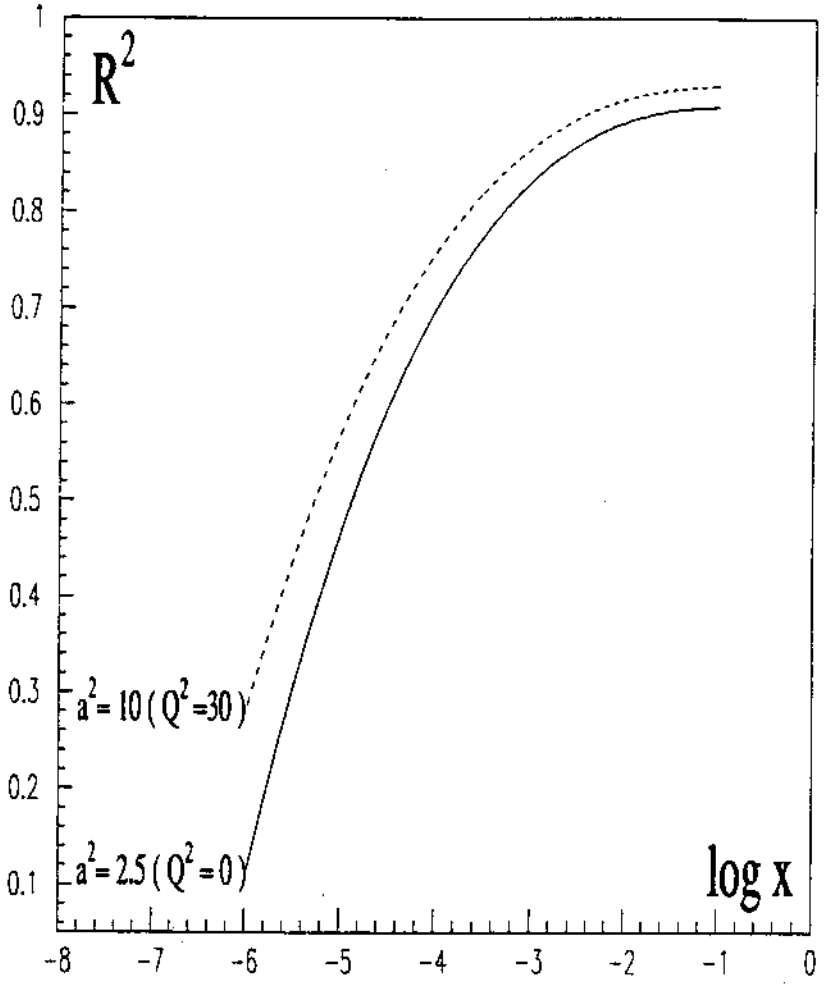

Figure 14: The ratio $R^2 = D_G^2(second\ iteration)/D_G^2(first\ iteration)$ for J/ψ production due to screening in the gluon distribution.

References

[1] J. Bartels and M. Loewe: *Z. Phys* **C 12** (1982) 263.

[2] E. M. Levin and M. G. Ryskin: *Phys.Rep.* **100** (1983) 1.

[3] A. Donnachie and P. V. Landshoff: *Phys. Lett.* **B185** (1987) 403; *Nucl. Phys.* **B311** (1989) 509.

[4] J. Bartels et.al.: *Phys. Lett.* **B348** (1995) 589.

[5] M. G. Ryskin: *Z. Phys.* **C57** (1993) 89.

[6] B. Z. Kopeliovich et.al.: *Phys. Lett.* **B324** (1994) 469.

[7] S. J. Brodsky et.al.: *Phys. Rev.* **D50** (1994) 3134.

[8] S. J. Brodsky and G. P. Lepage: *Phys. Rev.* **D22** (1980) 2157.

[9] A. H. Mueller: *Nucl. Phys.* **B335** (1990) 115;

[10] E. M. Levin and M. G. Ryskin: *Sov. J. Nucl. Phys.* **45** (1987) 150.

[11] B. Blättel et.al.: *Phys. Rev. Lett.* **71** (1993) 896.

[12] L. Frankfurt, G. A. Miller and M. Strikman: *Phys. Rev.* **D304** (1993) 1.

[13] E.Gotsman, E.M. Levin and U. Maor: *Phys. Lett.* **B353** (1995) 526.

[14] V. N. Gribov and L. N. Lipatov: *Sov. J. Nucl. Phys.* **15** (1972) 438; L. N. Lipatov: *Yad. Fiz.* **20** (1974) 181; G. Altarelli and G. Parisi: *Nucl. Phys.* **B 126** (1977) 298; Yu. L. Dokshitzer: *Sov.Phys. JETP* **46** (1977) 641.

[15] T. Jaroszewicz: *Phys. Lett.* **B116** (1982) 291.

[16] A. H. Mueller: *Nucl. Phys.* **B415** (1994) 373.

[17] N. N. Nikolaev and B. G. Zakharov: *Z. Phys.* **C49** (1991) 607; *Phys. Lett.* **B260** (1991) 414.

[18] L. N. Lipatov and V. S. Fadin: *Sov. Phys. JETP* **45** (1977) 199; Ya. Ya. Balitskii and L. V. Lipatov: *Sov. J. Nucl. Phys.* **28** (1978) 822; L. N. Lipatov: *Sov. Phys. JETP* **63** (1986) 904.

[19] M. Abramowitz and I. A. Stegun: Handbook of Mathematical Functions, Dover Publications,INC,New York 1970.

[20] E. M. Levin and M. G. Ryskin: *Phys.Rep.* **189** (1990) 267; *Sov. J. Nucl. Phys.* **50** (1989) 881; *Z. Phys.* **C48** (1990) 231.

[21] E. M. Levin, E. Gotsman and U. Maor: *Phys. Lett.* **B309** (1993) 109; *Z. Phys.* **C57** (1993) 667; *Phys. Rev.* **D49** (1994) R4321; *Phys. Lett.* **B347** (1995) 424.

[22] V. A. Abramovski, V. N. Gribov and O. V. Kancheli: *Sov. J. Nucl. Phys.* **18** (1973) 308.

[23] H. Abramowicz, L. Frankfurt and M. Strikman: DESY-95-047, March 1995.

[24] R. K. Ellis, Z. Kunszt and E. M. Levin: *Nucl. Phys.* **B420** (1994) 517.

[25] A. H. Mueller and J. Qiu: *Nucl. Phys.* **B268** (1986) 427.

[26] E. Levin and M. Wuesthoff: *Phys. Rev.* **D50** (1994) 4306.

[27] E. Laenen and E. Levin: *Ann. Rev. Nucl. Part. Sci.* **44** (1994) 199; CERN-TH/95-61, TAUP-22226-95,CBPF NF-012/95, March 1995.

[28] G. P. Lepage and S. J. Brodsky: *Phys. Lett.* **B87** (1979) 359.

[29] V. L. Chernyak and A. R. Zhitnitsky: *Phys. Rep.***112** (1984) 173.

[30] V. Braun and I. Halperin: *Phys. Lett.* **B328** (1994) 457.

[31] M. Gluck, E. Reya and A. Vogt: *Z. Phys.* **C53** (1992) 127.

[32] NMC Collaboration, P. Amaudruz et.al.: *Z. Phys.* **C54** (1992) 239.

[33] ZEUS Collaboration, M.Derric et.al.: DESY 95-133, July 1995.

[34] ZEUS Collaboration, M.Derric et.al.: DESY 95-052, March 1995.